Nonlinear phenomena in optical fibers

Halina Abramczyk

Technical University of Lodz, Laboratory of Laser Molecular Spectroscopy, 93- 590 Lodz, Wroblewskiego 15 str, Poland, abramczy@mitr.p.lodz.pl, www.mitr.p.lodz.pl/raman , www.mitr.p.lodz.pl/evu
Max Born Institute, Marie Curie Chair, 12489 Berlin, Max Born Str 2A, abramczy@mbi-berlin.de

4. Nonlinear phenomena

For many years the nonlinear phenomena were the matter of concern for relatively narrow circle of professionals dealing with the laser spectroscopy. So far, Raman scattering phenomena have widely been used in chemistry, materials engineering, and physics for research on the nature of interactions, chemical bonds and properties of semiconductors. During the last decade the interest in the stimulated Raman scattering and other nonlinear optical phenomena has significantly increased with the development of optical telecommunication. After 2000, almost all systems (long-haul – defined as ≈300 to ≈800 km and ultralong-haul – above 800km) have been using Raman amplification, substituting the most conventional in nineties EDFAs, erbium-doped fibre amplifiers. Despite the Raman amplification phenomenon had been demonstrated in optical waveguides by Stolen and Ippen in the beginning of seventies [1], the eighties and the former half of nineties were dominated by EDFA amplifiers. In the latter half of nineties the increase of interest in Raman amplifiers occurred. Evidently, the physics of Raman scattering phenomenon has remained the same since Raman and Krishnan publication in Nature in 1929 [2]. However, for the phenomenon to be applied there has to occur the significant progress in the optical waveguide technologies [3-5].

The radiation emitted by conventional light sources like electric bulbs, photoflash lamps, etc., is neither monochromatic nor coherent in time and space. Intensity of electric field of radiation emitted by conventional light sources is small (10-10^3 V/cm). Radiation of such intensity, when interacting with matter (reflection of light, scattering, absorption and refraction of light), does not change its macro- and microscopic properties, because it is several orders of magnitude smaller than the intensity of electric field in matter (of the order

of 10^9 V/cm). The intensity of laser light, in particular generated by pulse lasers emitting short pulses, can reach values of the order of 10^{12} W/cm^2 that corresponds to the intensity of the electric field of radiation of 10^5 to 10^8 V/cm. It is therefore comparable to the intensity of electric fields in matters.

Weak electric fields E of radiation generate electric induction D,

$$D = E + 4\pi P, \tag{4.1}$$

which depends on the polarisation of a medium P. For small values of light intensities, the polarisation is linearly related to the intensity of electric field E:

$$P = \chi^{(1)} E, \tag{4.2}$$

where $\chi^{(1)}$ - electric susceptibility.

The above formula arises from the fact that the medium polarisation P is a sum of orientation polarisation P^{orient} $\left(P^{\text{orient}} = N\frac{\mu^2}{3kT}E\right)$ and induced polarisation P^{ind} $\left(P^{\text{ind}} = N\alpha E\right)$.

If the intensity of the electric field E increases, the medium polarisation is no longer linearly dependent on E and should be expressed by the formula

$$P = \chi^{(1)}E + \chi^{(2)}E^2 + \chi^{(3)}E^3 + \ldots \tag{4.3}$$

For the correctness of notation, the above formula can be rewritten taking into account the fact that the electric susceptibility χ is not a scalar but a tensor:

$$P_i = \chi^{(1)}_{ij}E_j + \chi^{(2)}_{ijk}E_jE_k + \chi^{(3)}_{ijkl}E_jE_kE_l + \ldots \tag{4.4}$$

For the repeated subscripts of χ and the field intensity E, the summation over the x,y,z components of the field intensity should be done. If several weak electric fields act on a medium (e.g. a few leaser beams), the electric polarisation in a linear approximation is a sum of polarisation components of individual fields:

$$\mathbf{P}(\mathbf{r},t) = \mathbf{P}_1(\mathbf{r},t) + \mathbf{P}_2(\mathbf{r},t) + \mathbf{P}_3(\mathbf{r},t) + \ldots \tag{4.5}$$

It means that the weak electric fields meet the superposition principle, according to which the electromagnetic waves propagate in a medium independently, without mutual interaction. All the optical phenomena that can be approximated by that principle are called the linear optical phenomena. In case of strong electric fields the approximation (4.5) is not valid. The electric fields do not meet the superposition principle any longer. All the optical phenomena not meeting the superposition principle are called the nonlinear optical phenomena. An example of the nonlinear phenomenon is the dependence of the refractive index n on light intensity (Kerr effect). For low intensities of light the index is constant. However, if a medium is exposed to the light of the high intensity this is no longer valid and the refractive index is proportional to E^2 and makes liquids birefringent like crystals. Another example of linear phenomena is the absorption Lambert-Beer law

$$T = I / I_0 = \exp(-\alpha c l) \tag{4.6}$$

or

$$A = \ln\frac{1}{T} = \alpha c l, \tag{4.7}$$

where T is the transmittance of a system and it corresponds to the ratio of the output beam intensity I that went through the medium to the input beam I_0, α - absorption coefficient, c – concentration of substance absorbing the light, l –length of an optical path. Within the linear optics the absorption coefficient does not depend on light intensity. For higher light intensities the absorption coefficient does depend on that intensity.

4.1. Second-order nonlinear phenomena [6]

The second-order nonlinear phenomena are described by the second term of the equation (4.4):

$$P_i = \chi_{ijk}^{(2)} E_j E_k \qquad (4.8)$$

The most often employed second-order nonlinear phenomena are as follows: **a) second harmonic generation, b) frequency mixing, c) parametric amplification.** The detailed discussion of the second-order nonlinear phenomena can be found elsewhere [4].

The second harmonic generation can be exemplified by the following experiment. Let us direct a ruby laser light of the wavelength 694.3 nm on a nonlinear crystal. When we rotate the crystal, one can notice that at a specific angle between the direction of laser beam and the optical axis, the crystal output laser beam consists of two components: 694.3 nm and 694.3 nm/2 = 347.15 nm. Therefore, apart from the fundamental component 694.3 nm there appears additional component, called the second harmonic of the frequency twice as high as the fundamental (Fig. 4.3). The name of the process of the second harmonic generation can also be abbreviated to SHG.

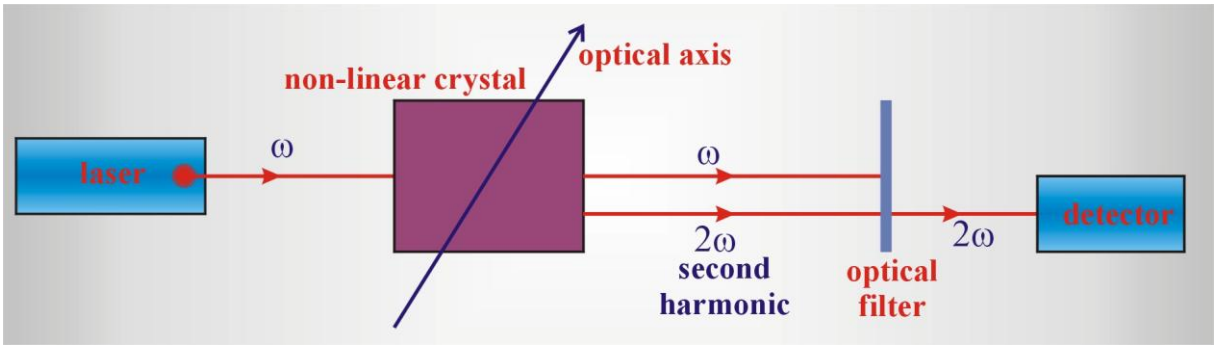

Fig. 4.1. Scheme of the second harmonic generation (SHG)

The second-order nonlinear phenomena are not so important in glass optical fibers. The silica glasses in contrast to crystals have amorphous structure with the inversion center and do not have the distinguished axis of symmetry. The inversion center simply means that the second – order term (4.8) disappears and SHG do not occur in glass optical fibers. The detailed description of the second-order nonlinear phenomena can be found in [4].

4.2. Third-order nonlinear phenomena [6]

One of the best known nonlinear optical phenomenon of the third-order is the stimulated Raman scattering. Raman scattering processes can be expressed by the following equation

$$P_i = \chi_{ij}^{(1)} E + \chi_{ijk}^{(2)} E_j E_k + \chi_{ijkl}^{(3)} E_j E_k E_l \,. \qquad (4.9)$$

The first term of the equation refers to the linear polarisation and depicts the spontaneous linear Raman scattering. The second term express the spontaneous nonlinear Raman scattering (hyperRaman scattering, HRS). The third term corresponds to the stimulated Raman scattering.

The spontaneous nonlinear Raman scattering has been described in a range of textbooks. The spontaneous Raman scattering can be outlined according to the scheme below(Fig. 4.2):

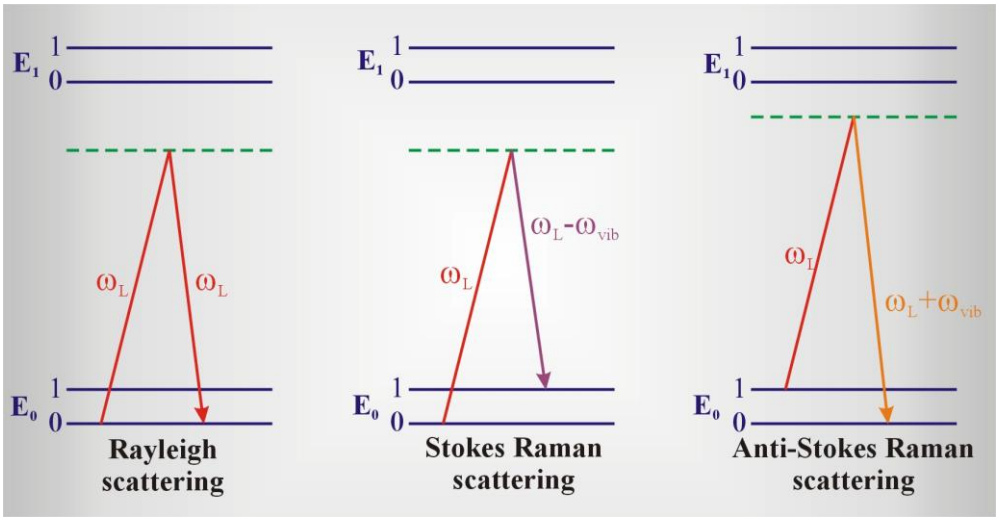

Fig. 4.2. Scheme of Rayleigh and Raman scattering.

E_0 and E_1 states correspond to the electronic states; the states enumerated with the quantum numbers υ denote the vibration states. When a photon of light with energy of $\hbar\omega_L$ which is lower than the resonance energy $\Delta E = E_1 - E_0$, falls onto a molecule, it undergoes the elastic or the inelastic scattering. The elastic scattering is called Rayleigh scattering, whereas the inelastic scattering – Raman scattering. The scattering process can be described classically. The electric field of the intensity $E_0\cos(\mathbf{k}\cdot\mathbf{r} - \omega_L t)$ produces the electron polarisation P of a medium that is time-modulated with the frequency of ω_L. Changeable over time the polarisation of medium induces the emission of electromagnetic waves of the same frequency ω_L (when dipole vibration are not modulated by vibrations of a molecule of the frequency ω_{wib}) or the frequency $\omega_L \pm \omega_{wib}$ (if the vibrations of dipole are additionally modulated by the vibrations of a molecule with the frequency of ω_{wib}). When the incident and scattered radiation frequencies are the same and equal ω_L, we call the phenomenon **Rayleigh scattering or elastic scattering**. When the frequency of the scattered radiation is lower $(\omega_L - \omega_{wib})$ or higher $(\omega_L + \omega_{wib})$ than the frequency of incident radiation ω_L. The scattered radiation of the frequency $\omega_L - \omega_{wib}$ is called the **Stokes Raman scattering** and that of the frequency $\omega_L + \omega_{wib}$ - **anti-Stokes Raman scattering**.

Quantum description can also be applied for the Raman scattering processes. The incident photon excites a molecule being in an electron state E_0 and a ground vibrational state (υ = 0) to a virtual state E that meets the condition $E_0 < E < E_1$. The lifetime of the molecule being in the virtual state is very short and afterwards it turns to: a) the initial state $(E_0, \upsilon = 0)$ that is accompanied by the photon emission of $\hbar\omega_L$ energy (Rayleigh scattering), b) the excited vibration state $(E_0, \upsilon = 1)$ emitting photons of energy

$\hbar(\omega_L - \omega_{wib})$ (Stokes Raman scattering) or c) if the $\hbar\omega$ photon irradiates a molecule in the electronic state E_0 and the excited vibration state $\upsilon = 1$, then it returns to the ground state $(E_0, \upsilon = 0)$ that is accompanied by the emission of the energy photon, $\hbar(\omega_L + \omega_{wib})$ (anti-Stokes Raman scattering). When the intensity of the incident radiation increases, the probability of the two photons Raman and Rayleigh scattering increases. Such phenomena are known as hyperRaman or hyperRayleigh (Fig. 4.3) and they are described by the second term of the (4.9).

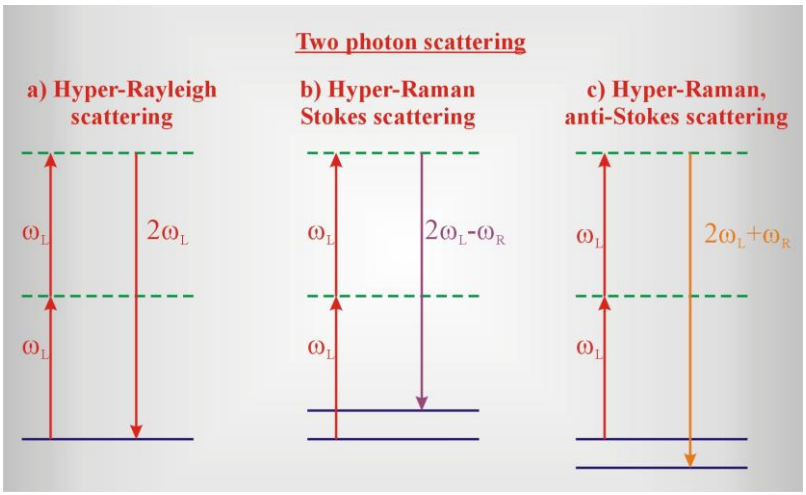

Fig. 4.3. Hyper-Rayleigh and hyper-Raman scattering

4.3. Stimulated Raman scattering (SRS)

The above described processes belong to the group of **spontaneous scattering** phenomena. Now, let us focus on the nonlinear third-order optical phenomena χ (3), which are responsible for the stimulated Raman scattering (the third term in (4.9)).

The scheme of quantum transitions in the stimulated Raman scattering (Fig. 4.4) does not differ from these in the spontaneous Raman scattering (Fig. 4.2).

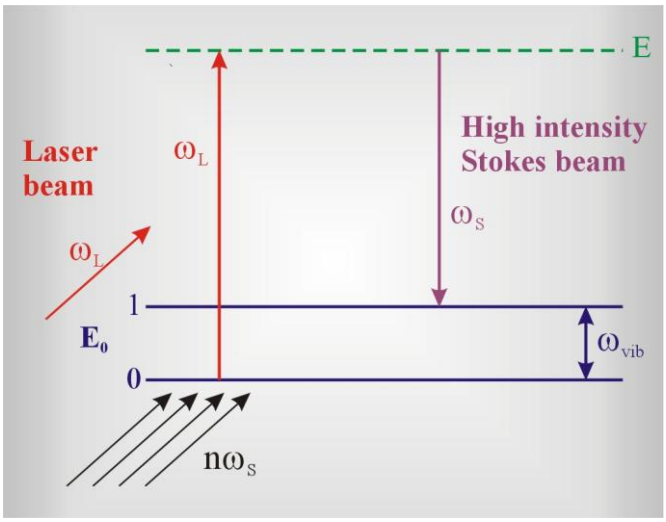

Fig. 4.4. Scheme of stimulated Raman scattering.

The difference is that the incident laser beam of the frequency ω_L characterised by the high intensity generates a strong Stokes beam $\omega_s = \omega_L - \omega_{wib}$. As a result the Stokes beam stimulates additional Stokes scattering from the virtual state E. This effect is analogous to the spontaneous and stimulated emission in a laser. The main difference is that absorption, spontaneous and stimulated emission occur between the stationary quantum states. For the incident and the scattered light of high intensity, two beams - ω_L and ω_s exist and interact with molecules of the system. This interaction leads to the generation of the phase coherent vibrations of the frequency $\omega_{wib} = \omega_L - \omega_s$. This denotes that all the molecules of the system vibrate in the same phase of the frequency ω_{wib}, because the effects of inter- or intramolecular interactions destroying the coherence are much lower than the strong interaction of a molecule with the electric fields of the beams ω_L and ω_s.

The stimulated anti-Stokes scattering is generated in a similar way. The spontaneous Raman scattering generates a weak anti-Stokes signal, since the population of the excited vibration levels is low according to the Boltzmann distribution. Illumination of a system with a high intensity ω_L beam leads to a perturbation of the Bolzmann distribution and as a result the stimulated anti-Stokes intensity increases significantly.

The stimulated Raman scattering is the special case of the four-wave interaction

$$\omega_4 = \omega_1 + \omega_2 \pm \omega_3, \tag{4.10}$$

$$\Delta\mathbf{k} = \mathbf{k}_1 + \mathbf{k}_2 \pm \mathbf{k}_3 - \mathbf{k}_4 = 0. \tag{4.11}$$

The equations (4.10) and (4.11) describe either three input $\omega_1, \omega_2, \omega_3$ beams and one output ω_4 beam interaction or two-fold interaction of the same beam like in the case of the stimulated Raman scattering. Indeed, the four-wave interaction for the stimulated Stokes scattering can be written as follows

$$\omega_4 = \omega_s = \omega_L - \omega_{wib} = \omega_L - (\omega_L - \omega_s) = \omega_L + \omega_s - \omega_L, \tag{4.12}$$

$$\text{thus, } \omega_4 = \omega_s;\ \omega_1 = \omega_L;\ \omega_2 = \omega_s;\ \omega_3 = -\omega_L. \tag{4.13}$$

The intensity of the stimulated Stokes scattering, I_S^w, can be expressed by the following formula

$$I_S^w = A \cdot \left(\chi^{(3)}\right)^2 I_L^2 I_s l^2 \left(\frac{\sin \Delta k l / 2}{\Delta k l / 2}\right)^2, \tag{4.14}$$

where: A – a constant, I_L and I_s - the intensities of the incident (pumping) and Stokes scattering beams, l – optical path length.

The anti-Stokes stimulated scattering can be written as a four-wave interaction

$$\omega_{AS} = \omega_L + \omega_{wib} = \omega_L + (\omega_L - \omega_s), \tag{4.15}$$

$$\text{thus} \quad \omega_4 = \omega_{AS};\ \omega_1 = \omega_L;\ \omega_2 = \omega_L;\ \omega_3 = -\omega_S. \tag{4.16}$$

The intensity of the stimulated anti-Stokes scattering, I_{AS}^w, is expressed by the equation

$$I_{AS}^w = A \cdot \left(\chi^{(3)}\right)^2 I_L^2 I_s l^2 \left(\frac{\sin \Delta k l / 2}{\Delta k l / 2}\right)^2. \tag{4.17}$$

The expressions (4.14) and (4.17) do not differ in the form, however, one should notice that the phase matching condition, Δk, varies for the Stokes and the anti-Stokes stimulated

scattering. The phase matching condition for the stimulated Stokes scattering takes the following form (4.12)

$$\Delta\mathbf{k} = \mathbf{k}_L + \mathbf{k}_S - \mathbf{k}_L - \mathbf{k}_S = 0, \qquad (4.18)$$

which indicates that the phase matching condition is satisfied for every propagation direction of the stimulated Stokes scattering. It means that the phase matching between the pumping beam, ω_L, Stokes beam, ω_s, and vibrations is achieved automatically.

In case of the anti-Stokes scattering the phase matching condition takes the form (4.15)

$$\Delta\mathbf{k} = \mathbf{k}_L + \mathbf{k}_L - \mathbf{k}_S - \mathbf{k}_{AS} = 2\mathbf{k}_L - \mathbf{k}_S - \mathbf{k}_{AS}. \qquad (4.19)$$

and the phase matching condition is only met for those directions that comply with the relation

$$\mathbf{k}_{AS} = 2\mathbf{k}_L - \mathbf{k}_S. \qquad (4.20)$$

It indicates that the direction of the stimulated anti-Stokes propagation is restricted to the surface of the cone with the axis parallel to the direction of the incident laser beam ω_L (Fig. 4.5).

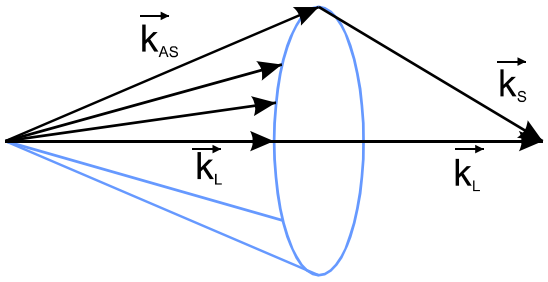

Fig. 4.5. Directions of propagation of the stimulated anti-Stokes scattering

Why the phase matching condition, $\Delta\mathbf{k} = 0$, that is always met for the stimulated Stokes scattering, it is not automatically complied with the stimulated anti-Stokes scattering? It results from the fact that the phase of vibrating molecules is defined by the more intense Stokes scattering.

To sum up, intense light of the frequency ω_L can cause intense stimulated Raman scattering: Stokes $\omega_S = \omega_L - \omega_{wib}$ and anti-Stokes $\omega_{AS} = \omega_L + \omega_{wib}$. As a result of photon interaction with matter, the energy exchange via optical phonons (or vibrations) takes place leading to the formation in a medium the third-order polarisation, $P^{(3)} \propto \chi^{(3)}_{ijkl} E_j E_k E_l$, that consists of the components changing with the frequency $\omega_{wib} = \omega_L - \omega_S$, $\omega_S = \omega_L - \omega_{wib}$ and $\omega_{AS} = \omega_L + \omega_{wib}$. The polarisation components generate new waves of the frequencies ω_S and ω_{AS} known as the stimulated Stokes and anti-Stokes Raman scattering. The phase matching condition is met in all directions for the Stokes radiation $(\Delta\mathbf{k} = 0)$, so the scattered light is emitted in all directions. The anti-Stokes stimulated scattering is observed in directions, $\mathbf{k}_{AS}$, for which the phase matching condition $2\mathbf{k}_L - \mathbf{k}_S = \mathbf{k}_{AS}$ is met.

The stimulated Raman scattering (SRS) produces both bad and beneficial effects in fibers. The essential feature of the stimulated Raman scattering is the **optical Raman gain.** If

in a medium, in which the stimulated Raman scattering occurs, two beams are guided: a beam called pumping beam of ω_L frequency and the additional one of the lower frequency equals to the Stokes component frequency $\omega_S = \omega_L - \omega_{wib}$ (propagating signal beam) the latter beam is significantly amplified. Therefore, we can expect the stimulated Raman scattering can be employed to amplify the input signal pulse in an optical fiber in a similar way as it undergoes in EDFAs, erbium-doped fibre amplifiers. The essential difference is the amplification of the propagating beam via the stimulated Raman scattering and the occurrence of the bathochromic shift (the Stokes component) $\omega_S = \omega_l - \omega_{vib}$ with respect to the pumping beam, where ω_{vib} denotes vibration frequency of the molecules of the fiber material (glass or dopants).

The Raman stimulated scattering in optical fiber can amplify weak propagating signal of frequency ω_s if the intense light is simultaneously pumped into a fiber with the frequency ω_L corresponding the amplification Raman spectrum $\omega_S = \omega_l - \omega_{vib}$. Maximum of amplification occurs only if the difference $\omega_S = \omega_l - \omega_{vib}$ equals to the maximum of the amplification Raman spectrum ω_{vib}. The amplification spectrum corresponds to the Raman vibration band of the fiber material. For the glass optical fiber ω_{vib} equals to 440 cm^{-1} (13.2 THz) and refers to the vibration of fused silica, SiO_2. The vibrational band of the fused silica is broad (around 5 THz) since glass is an amorphous, non-crystalline material and the spectrum is inhomogenously broadened. The amplification occurs when a threshold value for the stimulated Raman scattering is achieved.

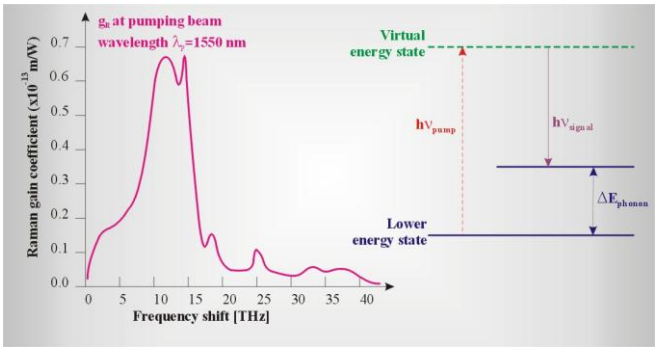

Fig. 4.6. Raman spectrum of melted silica SiO_2. The coefficient profile of the Raman amplification, g_R, pumping beam wavelength λ_p=1550 nm [7].

Let us consider an interaction between the pumping and the Stokes beams of the intensities I_p and I_s, respectively. Let us assume that they represent continuous waves CW (or quasi-CW). The intensities of the beams can be characterised by the following system of equations

$$\frac{dI_s}{dz} = g_R I_p I_s - \alpha_s I_s \qquad (4.21.a)$$

$$\frac{dI_p}{dz} = -\frac{\omega_p}{\omega_s} g_R I_p I_s - \alpha_p I_p \qquad (4.21.b)$$

The term $g_R I_p I_s$ depicts an increase in the intensity of the Stokes beam, where g_R refers to the spontaneous Raman scattering cross-section [8], (more precisely, imaginary part of the

third-order electric susceptibility $\chi^{(3)}_{ijkl}$ in the equation (4.9)), $\alpha_s\ \alpha_p$ - coefficients describing loses in an optical fiber for the Stokes and the pumping beams. One can accurately derive the equations (4.21.a - 4.21.b) from the Maxwell equations but they can also be intuitively understood as phenomenological equations. It becomes particularly clear for the case when the loses in the equation (4.21.b) are neglected, then we can write

$$\frac{d}{d_z}\left(\frac{I_s}{\omega_s}+\frac{I_p}{\omega_p}\right)=0 \tag{4.22}$$

This equation states that the total number of photons remains constant in the process of SRS.
In order to achieve the pumping beam I_p intensity threshold value, the set of equations (4.21.a - 4.21.b) has to be solved. To simplify the case, let us neglect the first term in the equation (4.21.b)

$$\frac{dI_p}{d_z}=-\alpha_p I_p \tag{4.23}$$

Solving the equation (4.23) and inserting to the equation (4.21a) we obtain

$$\frac{dI_z}{dz}=g_R I_0\ exp(-\alpha_p z)I_S-\alpha_S I_S \tag{4.24}$$

where I_0 denotes the intensity of pumping beam at the input, for z=0.
Solving the equation (4.24) we get

$$I_s(L)=I_s(0)\,exp\left(g_R I_0 L_{eff}-\alpha_s L\right) \tag{4.25}$$

where L denotes the length of an optical fiber, while L_{eff} is an effective length of an optical fiber

$$L_{eff}=\frac{\left[1-exp\left(-\alpha_p L\right)\right]}{\alpha_p} \tag{4.26}$$

The equation (4.25) says that at (z=0) where the pumping beam is injected the intensity of the signal beam is equal $I_s(0)$ and as a result of the stimulated Raman scattering is amplified to the value $I_s(L)$ when propagating along the length L. Here we assumed that during the process of SRS the photons of the frequency ω are generated. Indeed, SRS process amplifies all signals of the frequencies from the Raman band range (Fig. 4.6). Therefore the equation (4.25) should be substituted by the integration over whole Raman amplification band.

$$P_s(L)=\int_{-\infty}^{\infty}\hbar\omega\ exp\left[g_R\left(\omega_p-\omega\right)I_0 L_{eff}-\alpha_s L\right]d\omega \tag{4.27}$$

In order to solve the equation (4.27) the specific form of $g_R=g_R(\Omega)$ has to be known, where $\Omega=\omega_p-\omega$. Since usually the relation is not known, $g_R=g_R(\Omega)$ has to be expanded into Taylor series around the Stokes frequency $\omega=\omega_S$ and after substitution of the expansion we obtain

$$P_s(L)=P_{s0}^{eff}\ exp\left[g_R(\Omega_R)I_0 L_{eff}-\alpha_s L\right] \tag{4.28}$$

where

$$P_{s0}^{eff}=\hbar\omega_s B_{eff} \tag{4.29}$$

$$B_{eff}=\left(\frac{2\pi}{I_0 L_{eff}}\right)^{\frac{1}{2}}\left|\frac{\partial^2 g_R}{\partial\omega^2}\right|_{\omega=\omega_S}^{-\frac{1}{2}} \tag{4.30}$$

B_{eff} has the meaning of the effective Stokes bandwidth, and depends also on the pumping intensity and the fiber length L. The expression (4.29) can be treated as a good first-order approximation for estimation of the threshold power P_{s0}^{eff}, which is defined as the power of the Stokes beam power equal to the pumping power at the end of a fiber of the length L.

$$P_s(L) = P_p(L) \equiv P_0 \exp(-\alpha_p L) \tag{4.31}$$

where $P_0 = I_0 A_{eff}$ while A_{eff} denotes the effective surface of the optical fiber core defined by the equation:

$$A_{eff} = \frac{\left(\int_{-\infty}^{\infty} \int |F(x,y)|^2 dxdy \right)^2}{\int \int |F(x,y)|^4 dxdy} \tag{4.32}$$

For the Gaussian distribution of the beam the transverse area is

$$A_{eff} = \pi w^2 \tag{4.33}$$

where w denotes the width of the Gaussian distribution. The width w depends on the type of the propagated mode and a radius a of the core and the core and the cladding refraction indices. Fig. 4.7 shows the dependence of w/a on the normalized frequency discussed in Chapter 1

$$\upsilon = \frac{\pi a}{\lambda_0} \sqrt{\tilde{n}_1^2 - \tilde{n}_2^2} \ . \tag{4.34}$$

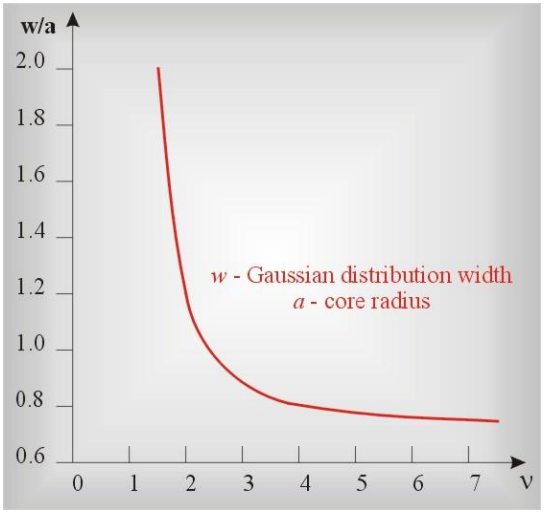

Fig. 4.7. Dependence of w/a on the normalized frequency υ

In the formula (4.34), the non-linearities generated by the high intensities of the fields of the stimulated Raman scattering has been taken into account by replacing the core and the cladding refraction indices n_1 and n_2 by their non-linear counterparts $\tilde{n}_1^2$ and $\tilde{n}_2^2$ in the formula (4.34). Therefore, within the nonlinear regime the nonlinear dielectric constants should be used

$$\varepsilon(\omega) = 1 + \chi_{xx}^{(1)}(\omega) + \varepsilon_{NL} \tag{4.35}$$

and as a consequence the nonlinear refraction index and the nonlinear absorption coefficient

$$\tilde{n} = n + n_2 |E|^2 \qquad \tilde{\alpha} = \alpha + \alpha |E|^2 \tag{4.36}$$

where

$$n_2 = \frac{3}{8n} Re\left(\chi^{(3)}_{xxxx}\right),\ \alpha_2 = \frac{3\omega_0}{4nc} Im\left(\chi^{(3)}_{xxxx}\right) \tag{4.37}$$

Fig. 4.8 describes the dependence of the refraction index of silica glass on the optical power. We can see that the changes are small, but for the great length of the optical fibers of the order of hundreds of kilometers this effect becomes meaningful.

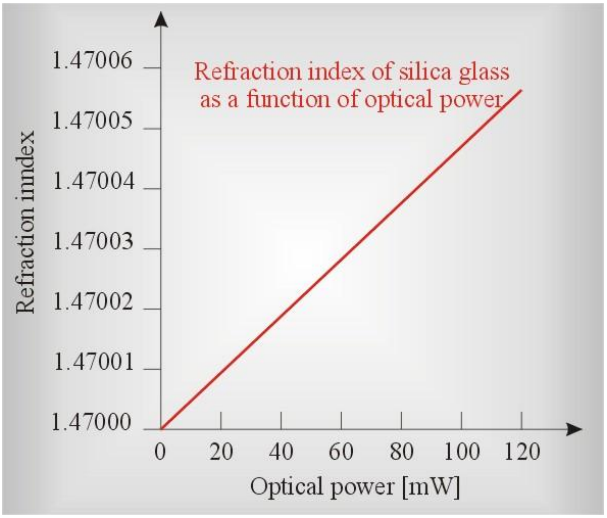

Fig. 4.8. Dependence of the refraction index of the silica glass on optical power.

Typical values of $n_2 \approx 2.6 \times 10^{-20} m^2 / W$ allow for the estimation of $A_{eff} \approx 20 - 100 \mu m^2$ for $\lambda_p = 1550nm$. Using the expression (4.28-4.31) allows us to write

$$P_{s0}^{eff}\ exp\left(\frac{g_R P_0 L_{eff}}{A_{eff}}\right) = P_0 \tag{4.38}$$

where P_{s0}^{eff} depends also on P_0 via the formula (4.29).

Assuming that the Raman gain spectrum, g_R, takes the Lorentz shape we get [9]

$$\frac{g_R P_0^{cr} L_{eff}}{A_{eff}} \approx 16 \tag{4.39}$$

Equation (4.39) allows deriving the threshold value P_0^{cr} above which the amplification phenomenon caused by the stimulated Raman scattering begins.

The stimulated Raman scattering phenomena have been used in Raman amplifiers. Since 2000 almost all systems (long-haul, defined as ≈ 300 to ≈ 800 km and ultralong-haul – over 800 km) have been using Raman amplification substituting popular in nineties EDFA amplifiers.

In typically applied configurations DFA (distributed fibre amplification) Raman amplification occurs at the end of the optical waveguide length, before detector or EDFA amplifier (Fig. 4.8). The pumping beam is inserted into an optical fiber through the coupler and propagates in the direction opposite to the direction of the signal beam.

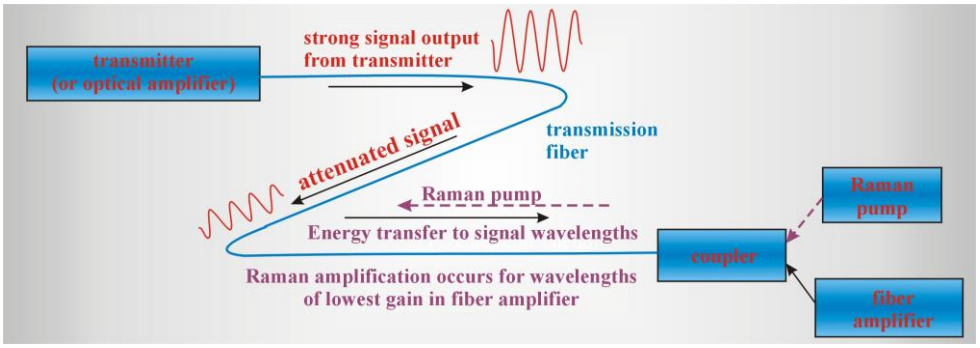

Fig. 4.8. Configuration DFA used in optical fibers with Raman amplification [3]

Fig. 4.6 shows the Raman spectrum for fused silica (SiO_2). It should be stressed that the maximum of the Raman vibrational band does not depend on the power of the signal beam. For fused silica, the Raman band of glass has the maximum at 13.2 THz (440 cm^{-1}). This means, if we use 1550 nm as the pumping beam, the bathochromic shift of 111.5 nm of the amplified Stokes beam (1661.5 nm), $\omega_S = \omega_p - \omega_{vib}$, will be observed. We will get the maximum of amplification for the same polarizations of the signal and the pumping beams.

The Raman amplifier is an example of benefits coming from the stimulated Raman scattering. However, SRS may create also many negative effects in the fiber. Here, some of them will be selectively described. It arises from the nature of the Raman phenomenon - higher frequency waves diminish their power as a result of energy transfer to optical photons and intermolecular vibrations, and the new Stokes waves of lower frequencies are created. This means that in an optical fiber, irrespective of our will, new longer wavelength components appear. If the power of light does not exceed a threshold value P_{th} (for typical optical waveguides of the order of 1W), radiation of longer wavelengths occurs as the spontaneous Raman scattering of low power. When the threshold value is exceeded, the stimulated Raman scattering appears at the cost of rapid decrease of the signal power. As long as the optical transmission is a single-channeled TDM with one wavelength propagating, the stimulated Raman scattering does not disturb significantly the operation of the system, although it influences the generation of noises coming from the stimulated Raman scattering. The situation changes dramatically in multi-channel broadband transmission (WDM). If two waves of frequencies ω_1 and ω_2 that differ by ω_{vib}, $\omega_2 = \omega_1 - \omega_{vib}$, the power of the longer wavelength λ_2 (signal wave) will increase at the cost of the power of the shorter wave λ_1 (pumping beam). This denotes that the channels of higher wavelengths will be amplified at the cost of the channels of lower wavelengths. It can lead to complete degradation of the multi-channel transmission system.

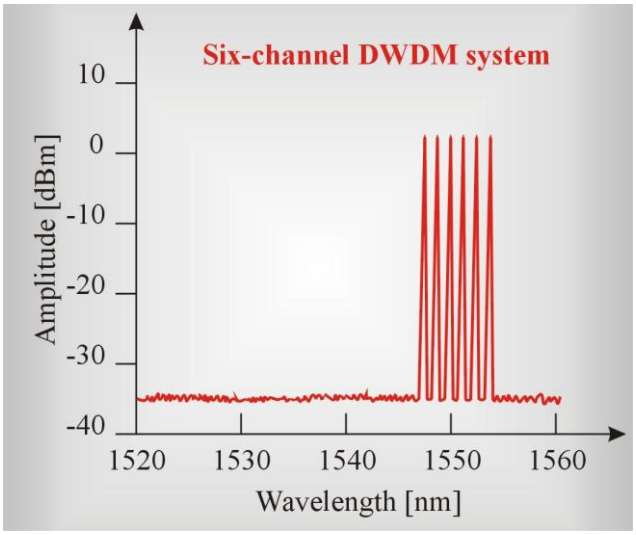

Fig. 4.9. Schematic spectrum for DWDM system that consists of six channels (six wavelengths) without the stimulated Raman effect.

Fig. 4.9 shows the spectrum of six-channel DWDM system (six wavelengths) at 1550nm window without the stimulated Raman scattering. Fig. 4.10 shows the deformation of the spectrum by the stimulated Raman scattering effect.

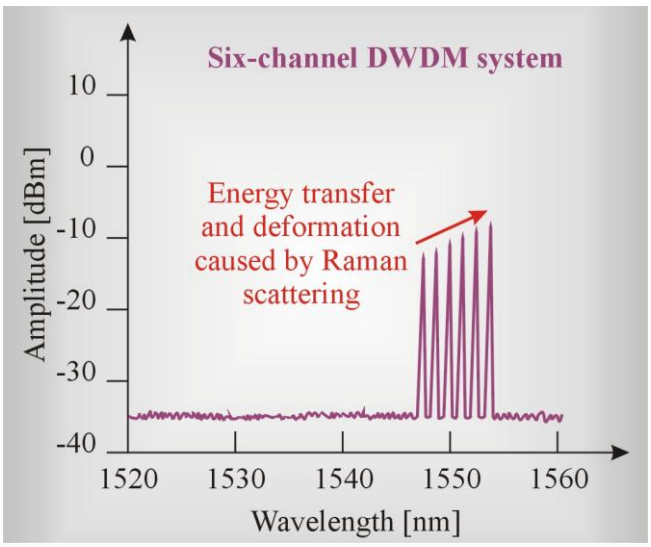

Fig. 4.10. Deformation of the spectrum for six-channel DWDM system (six wavelengths) by the stimulated Raman scattering effect.

Fig. 4.10 shows that the shorter wavelengths have significantly lower amplitudes due to the energy transfer to vibrations of the fused silica. The effect of mutual interaction of channels via SRS would be negligible only if the channels were separated by more than 13.2 THz corresponding to the maximum of Raman spectrum (that corresponds to silica vibration of 440 cm^{-1}). If a beam of 1550nm is used as pumping beam, the amplified Stokes beam $\omega_S = \omega_p - \omega_{vib}$ appears for wavelengths 113.6nm longer - at 1663.6 nm that corresponds to the channel spacing of 13.20 THz.

Figure 4.11 illustrates the influence of SRS on the binary signal transmission. The Fig. 4.11a shows a sequence of bits in two channels without the SRS effect. Fig. 4.11b shows

binary signals in both channels disturbed by SRS. It should be noticed that only when the value of a bit in any channel equals zero, SRS does not cause changes. If both channels emit nonzero bits, the power of the channel (λ_2) increases at the cost of the power of the channel (λ_1). In the channel (λ_1) the power of some bits decreases that leads to lower signal-to-noise ratio and in consequence to the increase of the **bit error rate**.

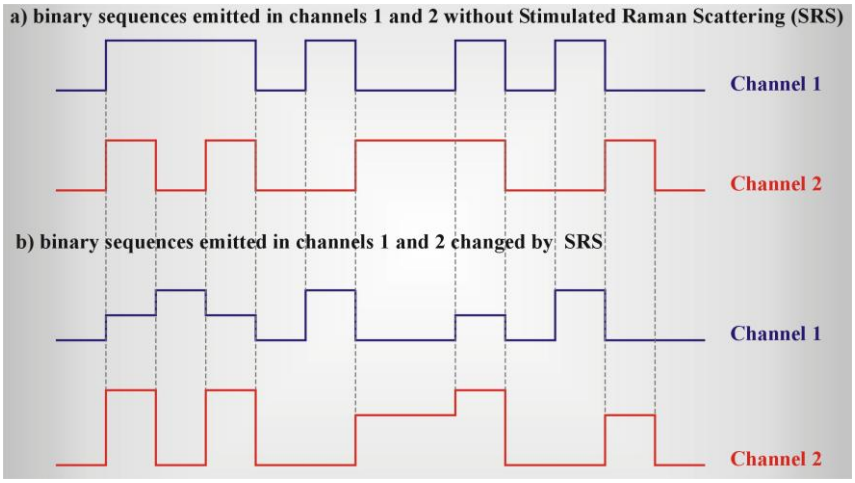

Fig. 4.11. Influence of SRS on transmission of binary signals, a) binary sequences emitted in channels 1 and 2 without SRS, b) binary sequences emitted in channels 1 and 2 and modified by SRS effect.

In order to restore the quality of the DWDM multi-channel transmission distorted by the stimulated Raman scattering effect (Fig. 4.10), the amplitudes of channels that transferred the energy to optical photons and vibrations, should be strengthened. It can be done applying Raman optical amplifiers. Fig. 4.8 shows DFA configurations of the Raman optical amplifier, with the backward pumping. In another configuration, the pumping laser and circulator are used (Fig. 4.12). The circulator injects light in opposite direction to the signal beam propagation.

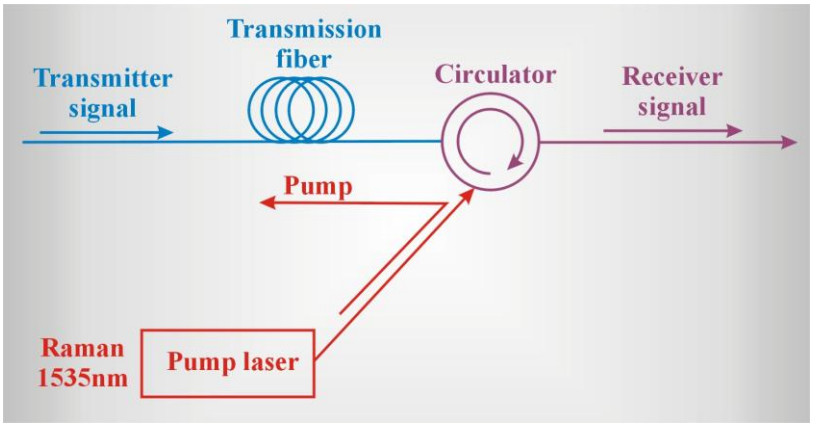

Fig. 4.12. Typical Raman amplifier configuration

Another solution is pumping in the same direction as the propagation of the signal beam (forward pumped Raman optical amplifier) with the pumping beam injected at the beginning of the optical tract in the neighborhood of the transmitter. The schematic spectrum from Fig. 4.10 after Raman amplification is presented in the Fig. 4.13. It can be noted that the pumping

beam power, 1535 nm, is much higher than the power of the components of the stimulated Raman scattering.

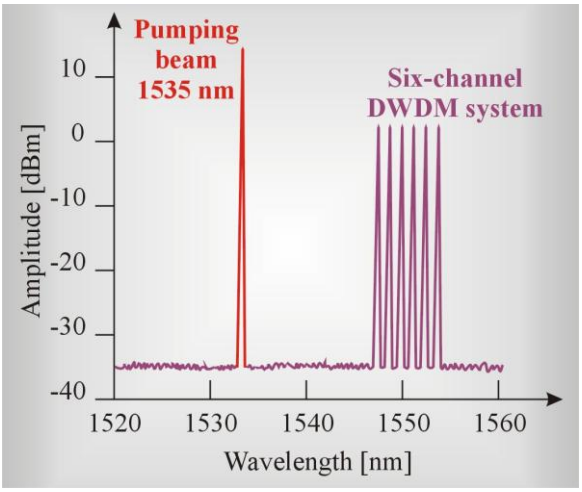

Fig. 4.13. Schematic representation of the Raman optical amplifier spectrum

When the Raman amplifier is used with the pumping light of 1535nm, all channels are amplified by about 10 dB (Fig. 4.14) and the amplitudes are again equal to each other (compare with Fig. 4.10). It happens at the cost of the energy of pumping beam at 1535nm, which is considerably lower (Fig.4.14) in comparison with situation in the Fig. 4.13.

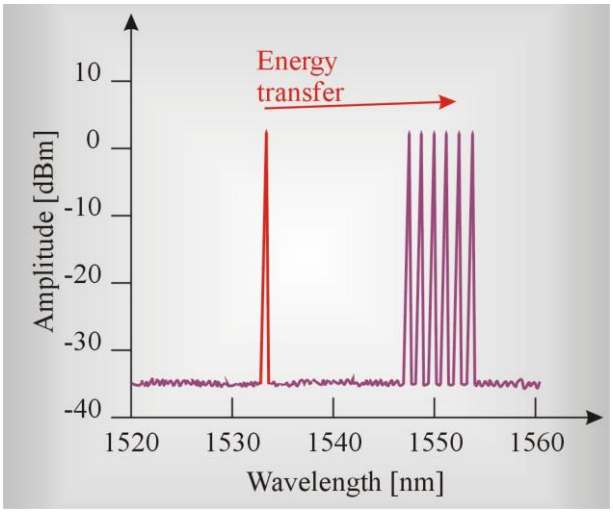

Fig. 4.14. Schematic representation of the spectrum of an example DWDM system that consists of six channels (six wavelengths) after amplification in the optical Raman amplifier; pumping at 1535nm

4.4. Stimulated Brillouin scattering

The Brillouin scattering and the stimulated Brillouin scattering can formally be described in a similar way as the Raman scattering. The wave of ω_L frequency can cause the Brillouin scattering as the Stokes component of frequency $\omega_S = \omega_L - \omega_{fa}$, where ω_{fa} denotes a frequency of an acoustic phonon. As a result of interaction between the matter and a

light photons the energy exchange occurs via acoustic photons leading to the third-order polarization of in medium, $P^{(3)} \propto \chi^{(3)}_{ijkl} E_j E_k E_l$. The fundamental difference lies in the interaction of light photons with acoustic phonons in contrast to the Raman scattering where the interactions between light photons and molecular vibrations occur. The acoustic phonons are of much lower frequencies than optical photons. The frequency of the acoustic phonon is expressed by the following formula

$$\omega_{fa} = \frac{4\pi n \upsilon_s}{\lambda} \tag{4.40}$$

where υ_s denotes the speed of sound in optical waveguide, n – refraction index. One can estimate the typical acoustic frequency from (4.40) which is equals to 69 GHz at wavelength of 1550nm.

The Brillouin scattering becomes the stimulated Brillouin scattering when the pumping threshold value is exceeded to generate the Stokes amplification. The bandwidth of the Brillouin amplification is much narrower than that of the Raman band and is equal approximately around $\Delta\nu_B$=20 MHz for 1550 nm. For comparison, the Raman amplification band is broad and equals around 5THz. This means that the highest amplification (the lowest threshold value) occurs for the sources of spectral bandwidth smaller than 20MHz. Indeed, the threshold value strongly depends on the spectral bandwidth of a light source. The more monochromatic source is, the lower the SBS amplification threshold is. For the very narrow spectral lines of 10MHz, the threshold value ranges from +4dBm to +6dBm for 1550nm. The Fig. 4.15 presents the dependence of threshold value on spectral line width of light source $\Delta\nu_L$. The broadening of the spectral line of a light source causes the reduction of the stimulated Brillouin effect.

$$g = g_B \frac{\Delta\nu_B}{\Delta\nu_L} \tag{4.41}$$

Calculations similar to those we carried out for the stimulated Raman scattering P_0^{cr} threshold value (4.38) allows to write [10]

$$P_0^{cr} = \frac{21 A_{eff}}{g_B L_{eff}} \tag{4.42}$$

Using the following parameters: L_{eff} =22 km, $A_{eff} = 50\mu m^2$, $g_B = 5 \times 10^{-11} m/W$, we get the threshold value for the stimulated Brillouin scattering $P_0^{cr} \approx 1$ mW. For such a threshold values the SBS is present and is the main nonlinear process in optical waveguides. The threshold value does not depend on the number of channels; it is present both in single (TDM) and multi-channel (WDM) transmission systems.

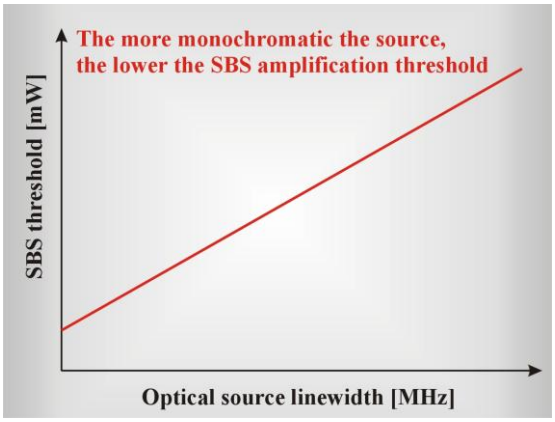

Fig. 4.15. The dependence of the threshold value on spectral line width.

Although the mechanisms of simulated Raman and Brillouin scattering are formally similar, there exist a few fundamental differences. First, the scattering amplification coefficient, $g_B \approx 4 \cdot 10^{-9} cm / W$, is twice as high as the corresponding coefficient for Raman scattering. It means a power of a few mW is enough for SBS effect production contrary to SRS where a power of above 200 mW causes SRS amplification. Second, contrary to Raman scattering, which propagates in both directions in an optical waveguide, Brillouin scattering propagates only in reverse direction in single-mode optical waveguides. Reverse process of Brillouin scattering degrades the transmitted signal. SBS phenomenon is very sensitive to the modulation of light. The higher the modulation speed, the broader spectrum of source $\Delta\nu_L$, so the lower amplification g_B (and higher the threshold value) that results from the equation (4.41) and allows for significant reduction of SBS.

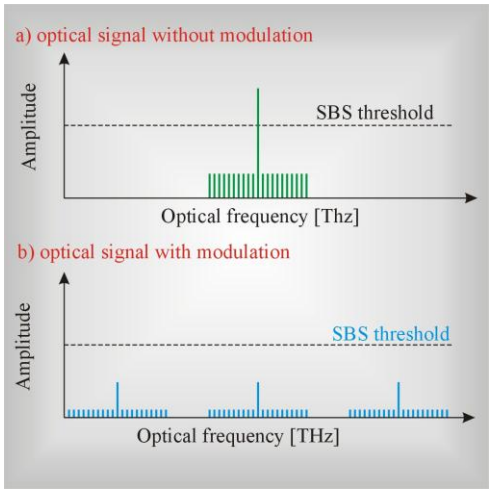

Fig. 4.16. Scheme of the influence of modulation on the threshold value of SBS, a) optical signal without modulation, b) optical signal with modulation.

4.5. Four-wave mixing (FWM)

The four-wave mixing is nonlinear process of the third order. This process is described by the third term in the polarisation expression

$$P_i = \chi_{ij}^{(1)} E + \chi_{ijk}^{(2)} E_j E_k + \chi_{ijkl}^{(3)} E_j E_k E_l \qquad (4.43)$$

As it has been shown in the chapter 3, the stimulated Raman scattering can be regarded as a special case of four-wave interaction

$$\omega_4 = \omega_1 + \omega_2 \pm \omega_3 \qquad (4.44)$$
$$\Delta\mathbf{k} = \mathbf{k}_1 + \mathbf{k}_2 \pm \mathbf{k}_3 - \mathbf{k}_4 = 0$$

Also the third harmonic generation is a special case of FWM, which appears when

$$\omega_1 = \omega_2 = \omega_3 \qquad (4.45)$$

and we obtain

$$\omega_4 = \omega_1 + \omega_1 + \omega_1 = 3\omega_1. \qquad (4.46)$$

In case of the single-channel optical transmission, the generation of the III harmonic is not a problem, since this nonlinear component can easily be filtrated, because it is in the spectral region significantly distant from the transmitted signal of ω_1 frequency. However, in the multi-channel systems with slightly different channel frequencies, the four-wave mixing leads to various combinations and some of them precisely overlap with the signal beam and the filtration becomes impossible. It is clear that the four-wave mixing is disadvantageous in transmission. Let us take into account three channels of wavelengths (λ_1, λ_2, λ_3). Let λ_1=1551.72nm, λ_2 = 1552.52 nm, and λ_3 = 1553.32 nm. The four-wave mixing process can lead to generation of signal of the following wavelengths

$\lambda_1+\lambda_2-\lambda_3$=1550.92nm	$\lambda_1-\lambda_2+\lambda_3$=1552.52nm	$\lambda_2+\lambda_3-\lambda_1$=1554.12nm
$\lambda_1-\lambda_2+\lambda_3$=1552.52nm	$2\lambda_1-\lambda_3$=1550.12nm	$2\lambda_2-\lambda_1$=1553.32nm
$\lambda_2+\lambda_3-\lambda_1$= 1554.12 nm	$2\lambda_3-\lambda 1$=1554.92 nm	$2\lambda_3-\lambda_2$= 1554.12 nm

Three of them are alike the signal wavelengths (Fig. 4.17), whereas the rest of six are different enough to filter them.

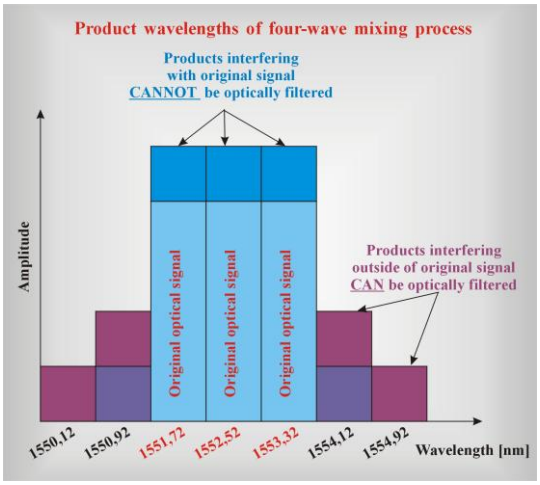

Fig. 4.17. Illustration of four-wave mixing phenomenon

The number of combinations of the interfering beams increases with the number of channels as ½ • (N^3-N^2) and is presented in Fig. 4.18.

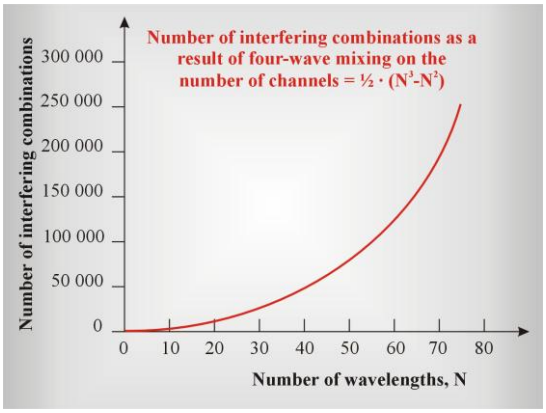

Fig. 4.18. The dependence of the number of interfering combinations as a result of the four-wave mixing on the number of channels.

The effectiveness of the four-wave mixing depends on the channel's frequency distance and dispersion characterised by the dispersion coefficient D that was discussed in chapter 3. The smaller the dispersion, the higher the four-wave mixing efficiency is. Therefore, in case of typical optical waveguides operating at 1310nm in the second window where D=0, the mixing is very efficient, whereas at 1550nm in the third window D=17 ps/nm•km and the four-wave mixing drastically decreases. For the new generation of dispersion shifted, low but non-zero-dispersion of the order of 1-5 ps/nm•km occurs to reduce the four wave mixing. The phenomenon is shown in Fig. 4.19.

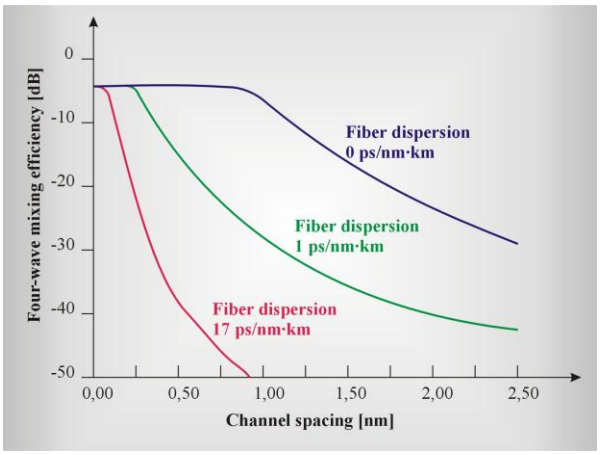

Fig. 4.19. Dependence of the four-wave mixing on the channel spacing

4.6. Self-phase modulation (SPM)

As an optical pulse travels down the fiber, the leading edge of the pulse causes the refractive index of the fiber to rise, resulting in a blue shift. The trailing edge of the pulse decreases the refractive index of the fiber causing a red shift. These red and blue shifts introduce a frequency chirp on each edge which interacts with the fiber dispersion and results in pulse broadening.

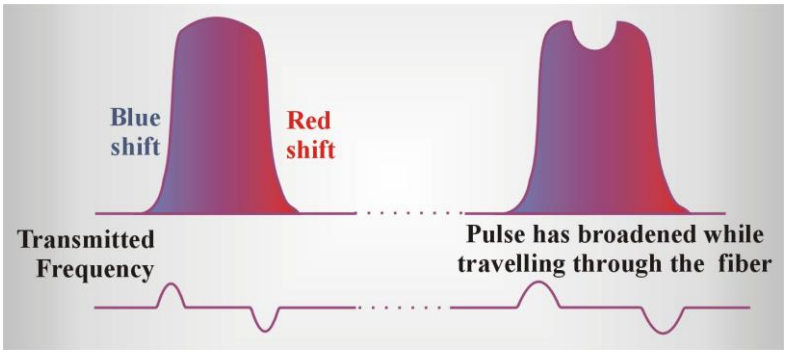

Rys.4.20. Pulse broadening in a fiber as a result of a frequency chirp

There is another effect which causes temporal broadening of an ultrashort pulse called the self phase modulation (SPM). This effect results from the fact that the nonlinear index of refraction n(ω) depends on the light intensity I

$$n(\omega) = n_0(\omega) + n_2(\omega)I(t) \tag{4.47}$$

$$I(t) = e^{-\Gamma t^2} \tag{4.47a}$$

When an ultashort pulse propagates through a nonlinear material the local index of refraction increases. The temporal center of the pulse, which is of course more intense, experiences a larger index of refraction than the leading and trailing edges. Therefore, the central part of the pulse slows, the leading edge speeds ahead, while the trailing edge catches up.
The nonlinear refraction index $n_2(\omega)I(t)$ leads to the time dependence of the phase

$$\phi = \beta L = \frac{n(\omega)\omega}{C} L = \frac{n_0(\omega) + n_2(\omega)I(t)}{C} \omega L$$

with its nonlinear part

$$\phi_{NL} = \frac{n_2(\omega)I(t)}{C} \omega L \tag{4.47b}$$

The time dependence of ϕ_{NL} results in the time dependence of the frequency along the temporal puls and differs from the central frequency ω_0 (Fig. 4.20). When the puls propagates in a fiber, its leading edge (with increasing intensity) experiences the frequency shift toward red wavelengths. In contrast, the trailing edge (or falling edge) with decreasing intensity experiences the frequency shift towards blue wavelengths. To understand, why it happens, one should be notice that the change of the frequency with respect to the central frequency $\delta\omega(T) = \omega - \omega_0$ is given by

$$\delta\omega(T) = -\frac{\partial\phi_{NL}}{\partial T}. \tag{4.47c}$$

Minus in the relation comes from the choice of the sign for the wave packet $exp(-i\omega_0 t)$, whereas T denotes time in the reference system moving with the group velocity of the wave packet maximum

$$T = t - \frac{2}{v_g} \tag{4.47d}$$

From (4.50) one can see that for the leading edge we have $\frac{\partial \phi_{NL}}{\partial T} > 0$ (because the nonlinear refraction index $n_2(\omega)I(t)$ increases) and $\delta\omega(T) < 0$, which denotes the red shift). In contrast for the trailing edge we have $\frac{\partial \phi_{NL}}{\partial t} < 0$ i $\delta\omega(T) > 0$ and the blue shift. As we can see from (4.50) the automodulation SPM generates new frequencies from the range $\omega_0 \pm \delta\omega(T)$ and results in spectral broadening of the puls. The time dependence of the frequency shift $\delta\omega$ is called the frequency chirping. When a puls propagates along the fiber ϕ_{NL} increases(because the distance *z* increases (4.49), and the frequency chirp $\delta\omega$ also increases. It indicates that with the distance new frequencies are generated in the propagating puls which becomes more and more spectrally broadened. This phenomenon is of spectral broadening resulting from the nonlinearity of the refraction index ($n_2(\omega)I(t)$) is known as the automodulation SPM. The spectral broadening leads to the temporal pulse broadening. SPM effect on the pulse duration seems to run counter to accepted ways of thinking: the broader the pulse in the frequency domain, the shorter the pulse in the time domain. To understand this apparent discrepancy with the Fourier transformation we have to stress that the new frequencies created by SPM are not synchronized. Although they are produced under the original pulse envelope, they are not transform-limited any longer as the pulse propagates

It should be remembered that to the SMP effect we must add the group velocity dispersion efect GVD described in chapter 3. In medium exhibiting positive „normal" efect GVD (GVD>0) red spectral components travels faster than blue components. Each of them undergoes additional dispersion resulting from the automodulation. It denotes that the red components on the leading edge becomes further shifted to red (and blue) and the blue components on the trailing edge are further shifted towards blue (and red).

To sumarize, the automodulation SMP, particularly when combined with positive GVD, leads to both spectral and temporal pulse stretching

The Fig. 4.21 shows the temporal phase change Φ_{NL} resulted form self-phase modulation (a) and frequency chirp for Gaussian (m=1) and super-Gaussian (m=3) temporal pulse.

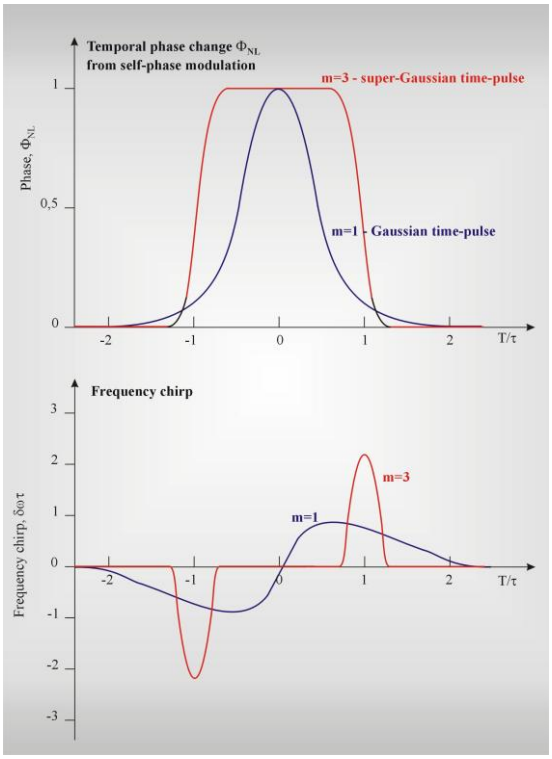

Fig. 4.21. Temporal phase change Φ_{NL} resulting from self-phase modulation (a) and frequency chirp for Gaussian (m=1) and super-Gaussian (m=3) temporal pulse [15]

As a consequence of the phenomenon presented in the Fig. 4.21, temporal broadening of a pulse appears. The Fig 4.22 demonstrates the dependence of the self-phase modulation on the pulse broadening for the following cases (a) the input pulse without chirp, (b) the same pulse after distance L in the optical fiber, (c) the input pulse with chirp, (d) the same pulse with input chirp after distance L in the optical fiber.

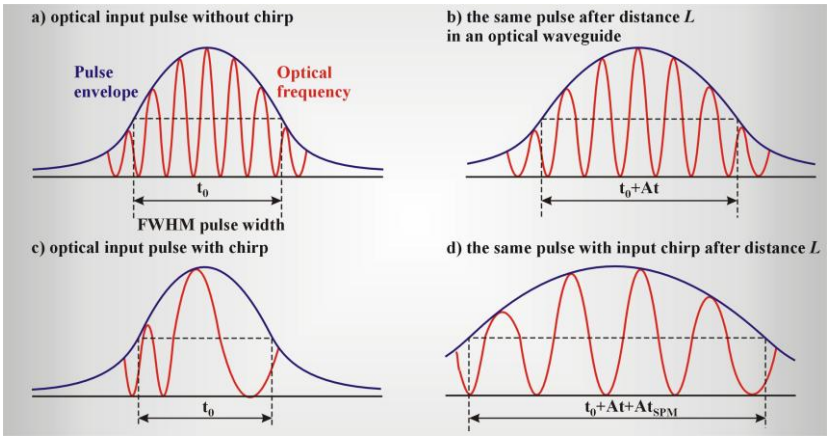

Fig. 4.22. Dependence of the self-modulation on broadening of the temporal pulse (a) input unchirped pulse (b) the same pulse after the distance L in optical fiber (c) input chirped pulse, (d) the same pulse with input chirp after the distance L in optical fiber

When the intensity of the pulse increases, the temporal pulse not only broadens but also gains an oscillatory character. The oscillatory character can be understood when we take into account the changes of frequencies during the pulse durations (Fig. 4.21).

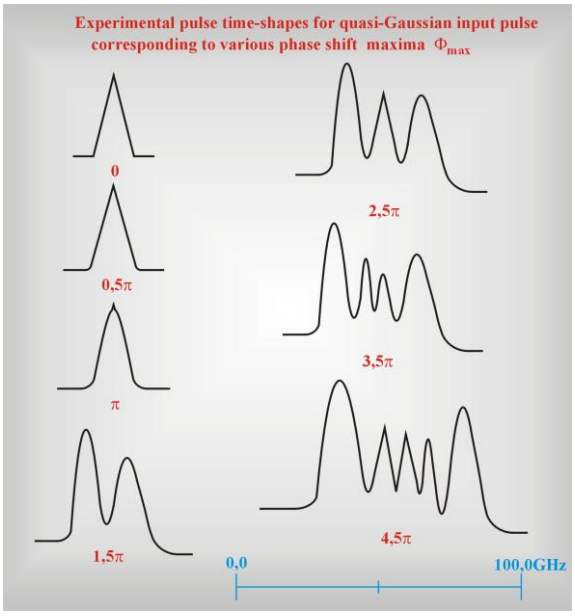

Fig. 4.23. The shape of time pulses experimentally observed in case of quasi-Gaussian input pulse after travelling the distance of 99 m in an optical waveguide (a=3.35 μm, V=2.53). Various shapes correspond to the various maxima of the phase shift Φ_{max} that is proportional to the pulse power, time duration of the input pulse $\tau_0 \approx 90 ps$ [11].

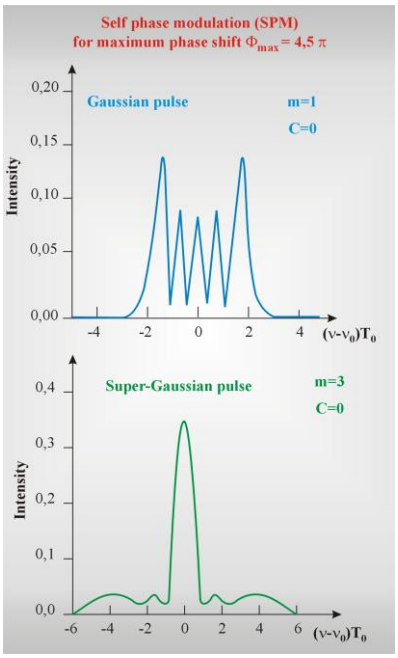

Fig. 4.24. Comparison of influence of SPM on the time shape of pulse for the input pulse (a) Gaussian and super-Gaussian (b) and for the power P_0 corresponding to maximal phase shift $\Phi_{max} = 4.5\pi$ [12].

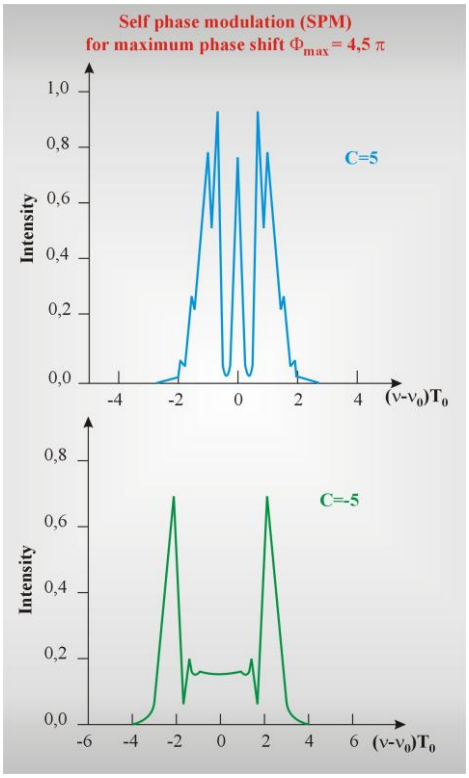

Fig. 4.25. Comparison of influence of SPM on the time shape of pulse for the input pulse with positive GVD (C=5) (a) with the negative GVD (C=-5) and for the power P_0 corresponding to the maximal phase shift $\Phi_{max} = 4.5\pi$ [13].

If an input pulse is accompanied by the initial chirp the temporal pulse shows even more spectacular character (Fig. 4.25) with clear oscillatory character for the positive GVD (C=5). Contrary, if the input pulse shows negative dispersion (C=-5), the oscillatory character decays in the middle of the pulse leaving only two pulses on the edges.

However, the SPM effect can also play a positive role. It can be used to compress ultrafast pulses. Two general techniques are used to compress ultrafast pulses via SPM and GVD combination: a) the grating-fiber method, b) the soliton-effect compressor. The first method is used in the visible and the near infrared ranges. The second method is used in fiber networks. The principle of the grating-fiber method is presented in fig. 4.26. First, recall that for most wavelengths, materials show so-called "normal dispersion" (GVD>0) , where the index of refraction n increases as λ decreases (Fig. 3.10). However, for the wavelengths that are close to the maximum of the absorption band, the dependence of the index of refraction on wavelength λ changes - the index of refraction n increases as λ increases (Fig.3.11). At the center of absorption, the GVD is zero. The material shows so-called "anomalous dispersion" close to the maximum of the absorption, and the pulse exhibits a negative GVD, with the bluer components of the pulse traveling faster than the redder components. The grating-fiber method is used for VIS and near-IR pulses that are far from the absorption band of the fiber material. Let the input pulse represents the normal dispersion region with a positive GVD. During the propagation in the fiber the pulse is affected both by SPM and GVD. The resulting pulse has its spectral width significantly increased with a significant positive chirp, which is almost linear. Then, the positively chirped pulse passes through an external pair of gratings, which are designed to produce negative GVD. The negative GVD designed pair of grating offset the positive chirp from the positive GVD and SPM by making the optical path length of the redder components substantially greater than the path for the bluer components.

Therefore, the trailing bluer edge of the pulse catches up to the leading redder edge, and all components begin to travel at the same velocity. As a result, the output pulse exhibits zero GVD, and is compressed to less than its initial value.

The soliton-effect compressor is used for radiation close to the absorption band of the fiber material. The silica fiber has the absorption (and zero GVD) at 1.31 μm. Therefore, for radiation close to the maximum the fiber exhibit anomalous dispersion, and the pulse propagating across the fiber experience a negative GVD. The soliton-effect compressor consists simply of a piece of fiber of properly chosen length to balance the positive chirp introduced by SPM with the negative chirp introduced by the fiber. These two effects together can offset each other in a properly chosen fiber length and the result is a compressed pulse that exhibits zero GVD. This pulse is called an optical soliton. Such a pulse is stable in shape, power and duration over extremely long distances and can be transmitted in telecommunication optical fibers without distortion.

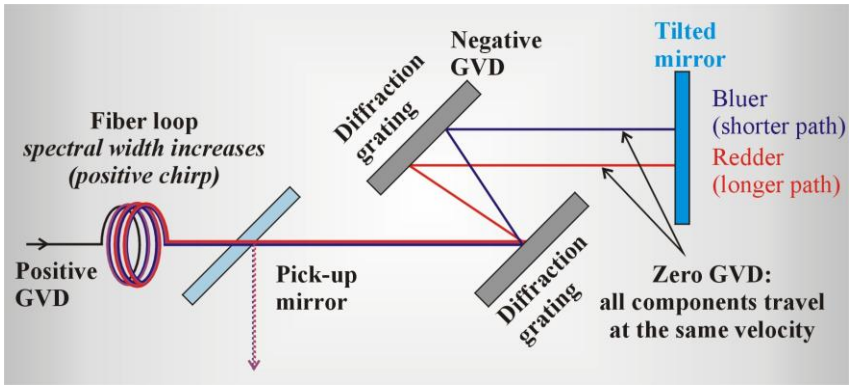

Fig. 4.26. Typical setup for the grating-fiber compression

These effects are present both in solid-state lasers based on a crystal medium as well as in fiber lasers with a silica glass as a laser medium. The silica glass has a symmetry center of inversion that rules out the second-order nonlinear effects, but the third order effects like SPM still exists. SPM effect in fiberoptic systems is smaller than in solid-state lasers, because of significantly smaller intensities that are employed.

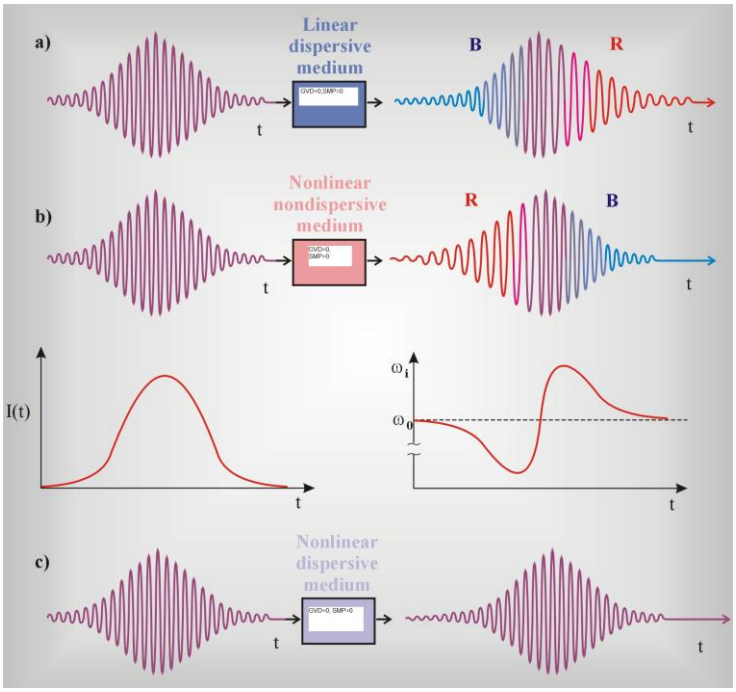

Fig.4.27. SMP and GVD effects on the temporal pulse shape and duration, a) (GVD<0; n_2 =0, SMP=0), b) (GVD=0; n_2>0, SMP>0),c) (GVD<0; n_2>0, SMP>0)

Fig. 4.27 summarizes the discussion on the SMP and GVD effects and their inluence on the temporal pulse shape and duration

a) when the non-chirped input pulse propagates in the medium exhibiting the negative GVD and no SMP effect (GVD<0; n_2 =0 from eq. (4.47) the pulse at the end of the fiber becomes negatively chirped with the shorter wavelengths (B components in Fig. 4.27) traveling faster than the longer spectral components (R components) of the pulse,
b) when the non-chirped input pulse propagates in the medium exhibiting no GVD dispersion, but SMP effect exists (GVD=0; n_2 >0 from eq. (4.47) the pulse at the end of the fiber shows blue shift (R components) for the raising edge of the pulse and red shift (B components) for the trailing edge, the pulse shows frequency chirp, but the shape remains unchanged,
c) when the output pulse from the case b) will be employed as the input pulse in the case a), the pulse undergoes narrowing,
d) when the non-chirped input pulse propagates in the medium exhibiting negative GVD dispersion, and SMP effect exists (GVD<0; n_2 >0 from eq. (4.47) the pulse at the end of the fiber can preserve their shape and duration (solitons) or change the shape. Both cases- broadening or narrowing can be obtained depending on competition between GVD and SMP effects.

4.7. Cross phase modulation (XPM)

The cross-phase modulation (XPM) is very similar to SPM except that it involves two pulses of different frequency, whereas SPM involve the pulses of identical frequency. In XPM, two pulses travel along the fiber, each changing the refractive index

$n_L(\omega)I(t)$ as the optical power increases. If these two pulses happen to overlap, they will introduce distortion into the other pulses through XPM. In contrast to SPM, the fiber dispersion has little impact on XPM. Increasing the fiber effective area reduces XPM and all other fiber nonlinearities.

4.8. Theoretical description of GVD phenomenon and self-phase modulation SPM [14,15]

4.8.1. Nonlinear Schrodinger equation

Polarization controls matter-radiation interaction, therefore it plays significant role in description of phenomena occurring in optical waveguides.

Polarization operator for N molecules is described with the equation

$$\hat{P}(\boldsymbol{r}) = \sum_m P_m(\boldsymbol{r}) \tag{4.49}$$

where $P_m(\mathbf{r})$ polarization of molecule m

$$P_m(\boldsymbol{r}) = \sum_\alpha \int_0^1 du\, q_{m\alpha}(\hat{r}_{m\alpha} - R_m)\delta[\boldsymbol{r} - R_m - u(\hat{r}_{m\alpha} - R_m)] \tag{4.50}$$

Here, $\hat{r}_{m\alpha}$ is the position operator, q_{ma} is the electric charge of particle □ (electron or nucleus) belonging to molecule m, R_m is a molecular center of mass (or charge), the u–integration is a number integration that ensures the correct coefficients of the multipolar expansion of the polarization operator.

Most commonly we shall invoke the dipole approximation where we keep only the first electric term in the multipolar expansion. The equation (4.50) is then simplified to the form

$$\hat{P}(\boldsymbol{r}) = \sum_m \mu_m\, \delta(\boldsymbol{r} - \boldsymbol{R}_m) \tag{4.51}$$

where μ_m is the dipole moment operator for the m^{th} molecule and is given by

$$\mu_m = \sum_\alpha q_{m\alpha}(\hat{r}_{m\alpha} - R_m). \tag{4.52}$$

The $\delta(r - R_m)$ is the Dirac delta function

$$\delta(r - R_m) = \begin{cases} \infty & r = R_m \\ 0 & r \neq R_m \\ \int f(r)\,\delta(r - R_m)dr = f(R_m) \end{cases} . \tag{4.53}$$

The electric field of the laser $\boldsymbol{E}(\boldsymbol{r},t)$ interacts with the matter through the polarization $\boldsymbol{P}(\boldsymbol{r})$. The radiation-matter interaction is given by the semiclassical Hamiltonian

$$H_{int}(t) = -\int E(\boldsymbol{r},t)P(\boldsymbol{r})d\boldsymbol{r} \quad (4.54)$$

The radiation-matter interaction described by eq. (4.54) can be simplified if we assume the dipole approximation (eq. (4.51)). The dipole approximation denotes that a single particle has a size much smaller than the optical wavelength and the particle may be represented by a point dipole. When the dipole approximation is made we can focus on the temporal response of a single particle to the electric laser field and the Hamiltonian H_{int} from (eq.(4.54)) can be written as

$$H_{\text{int}}(t) = -\boldsymbol{E}(\boldsymbol{r},t)\boldsymbol{V}, \quad (4.55)$$

with the dipole operator

$$\boldsymbol{V} = \sum_{\alpha} q_{\alpha}(\boldsymbol{r} - \boldsymbol{r}_{\alpha}) \quad (4.56)$$

where the sum runs over all the electrons and nuclei a with charges q_a at positions $\boldsymbol{r}_{\alpha}$.

In the semiclassical description of the interaction the material system is treated quantum mechanically whereas the transverse radiation field $\boldsymbol{E}(\boldsymbol{r},t)$ is considered classical.

In the Schrödinger picture, the semiclassical approximation results in the Maxwell-Liouville equations:

$$\nabla \times \nabla \times E(\boldsymbol{r},t) + \frac{1}{c^2}\frac{\partial^2}{\partial t^2}E(\boldsymbol{r},t) = -\frac{4\pi}{c^2}\frac{\partial^2}{\partial t^2}P(\boldsymbol{r},t) \quad (4.57)$$

$$P(\boldsymbol{r},t) = Tr\left[\hat{P}(\boldsymbol{r})\,\rho(t)\right] \quad (4.58)$$

$$\frac{\partial \rho(t)}{\partial t} = -\frac{i}{\hbar}\left[H_T, \rho(t)\right] \quad (4.59)$$

The dynamics of the system is calculated by solving coupled equation for the electric field and the polarization. As we said, the optical polarization $P(\boldsymbol{r},t)$ is the primary goal of any theory of optical spectroscopy because it plays a key role for interpreting optical measurements. To calculate the polarization $P(\boldsymbol{r},t)$ which is a physical observable we have to average over the statistical ensamble (eq. (4.58)) with the nonequilibrium density operator $\rho(t)$ by taking a trace Tr. The density operator $\rho(t)$ can be obtained by solving the Liouville equation (4.59) where H_T is given by

$$H_T = H + H_{\text{int}} \quad (4.60)$$

and describes the Hamiltonian H of the molecular system (matter) and the Hamiltonian of interaction matter-radiation H_{int} given by eq. (4.54).

Unfortunately, the equation (4.59) is easy to solve only for the thermal equilibrium ($t=t_0$) when the electric field of the laser does not disturb the system ($H_{int}=0$) and the canonical density operator is given by

$$\rho(t_0) = \rho(-\infty) = \frac{exp(-\beta H\ )}{Tr\,exp(-\beta H)} \quad (4.61)$$

where $\beta = (k_B T)^{-1}$, k_B is the Boltzman constant, and T is the temperature.

For nonequilibrium situation, when the laser beam begins to interact with the molecular system, the eq. (4.59) is not easy to solve. Usually, a perturbative order by order expansion of the response in the fields is applied which indicates that the time-dependent density operator can be expanded in powers of the electric fields

$$\rho(t) = \rho^{(0)}(t) + \rho^{(1)}(t) + \rho^{(2)}(t) + \rho^{(3)}(t) + \ldots \quad (4.62)$$

where $\rho^{(n)}$ denotes th n^{th} order contribution in the electric field, $\rho^{(0)}(t) = \rho(-\infty)$.
Upon the substitution (4.62) into (4.58) we obtained the Taylor expansion of the polarizaion in powers of the radiation field $E(\boldsymbol{r},t)$

$$P(\boldsymbol{r},t) = P^{(1)}(\boldsymbol{r},t) + P^{(2)}(\boldsymbol{r},t) + P^{(3)}(\boldsymbol{r},t) + \ldots \quad (4.63)$$

As we explained in chapter 5 this expansion corresponds to the linear and nonlinear optical processes. The linear term $P^{(1)}$ is responsible for linear optics, $P^{(2)}$ is responsible for second-order processes such as SHG or frequency sum generation, $P^{(3)}$ is the third-order polarization that is responsible for THG and many other processes that is measured by a broard variety of laser techniques such as four-wave mixing, pump-probe spectroscopy or polarization-gating. It can be shown [9.6] that the n^{th} order polarizability $P^{(n)}(\boldsymbol{r},t)$ is expressed by the n^{th}-order nonlinear response functions $S^{(n)}$ that provide the complete information about the time evolution of the system measured by the optical spectroscopy of the n^{th} order and is given by [9.6]:

$$P^{(n)}(\boldsymbol{r},t) = \int_0^\infty dt_n \int_0^\infty dt_{n-1} \ldots \int_0^\infty dt_1 S^{(n)}{}_{t_n,t_{n-1},\ldots,t_1} E(\boldsymbol{r},t-t_n) E(\boldsymbol{r},t-t_n-t_{n-1}) \ldots E(\boldsymbol{r},t-t_n-t_{n-1}-\ldots t_1) \quad (4.64)$$

where the response function $S^{(n)}$ is given by

$$S^{(n)}(t_n,t_{n-1},\ldots,t_1) = \left(\frac{i}{\hbar}\right)^n \theta(t_1)\theta(t_2)\ldots\theta(t_n) \times \langle V(t_n+\ldots+t_1)[V(t_{n-1}+\ldots+t_1),[\ldots[V(t_1),[V(0),\rho(-\infty)]]\ldots]]\rangle \quad (4.65)$$

Here $\theta(\tau)$ is the Heavyside step function [$\theta(\tau)=1$ for t>0 and $\theta(\tau)=0$ for t<0], $\rho(-\infty)=\rho_0$ represents the equilibrium density operator, which does not evolve with time only when the molecular Hamiltonia H does not interact with electric field of the laser. The operator V(t) from eq. (4.65) can be expressed as

$$V(\tau) = \exp\left(\frac{i}{\hbar}H\tau\right) V \exp\left(-\frac{i}{\hbar}H\tau\right) \quad (4.66)$$

and represents the dipole operator from eq. (4.56) in the interaction picture. One can see from eqs. (4.64-4.66) that the polarization response $P^{(n)}$ is expressed by the n-time points correlation functions.

For the linear response $P^{(1)}$ that controls all linear spectroscopy optical measurements (for example absorption, spontaneous Raman scattering) the response function $S^{(1)}$ is simplified to the from

$$S^{(1)}(t_1) = \frac{i}{\hbar}\theta(t_1)\langle[V(t_1),V(0)]\rho(-\infty)\rangle \quad (4.67)$$

and represents well known two-points correlation functions. These functions describe dynamics of vibrational relaxation in IR and Raman spectroscopy through the vibrational correlation function $\langle Q(t)Q(0)\rangle$ and dynamics of reorientational relaxation. The higher-order response functions are a little more complicated, but at some approximations they can be

factorized and expressed as a product of two-time point correlation functions. The exact form of various responses for a specific nonlinear spectroscopy, including pump-probe, polarization-getting, echoes, coherent Raman the reader can find in Mukamel's book [14].

The equation (4.57) simplifies to the following wave equation

$$\nabla^2 E(\boldsymbol{r}, t) - \frac{1}{c^2}\frac{\partial^2 E(\boldsymbol{r}, t)}{\partial t^2} = \mu_0 \frac{\partial^2 P_L(\boldsymbol{r}, t)}{\partial t^2} + \mu_0 \frac{\partial^2 P_{NL}(\boldsymbol{r}, t)}{\partial t^2} \tag{4.68}$$

where $P_L(\boldsymbol{r}, t)$ and $P_{NL}(\boldsymbol{r}, t)$ are linear and non-linear polarization, accordingly, so $P_L(\boldsymbol{r}, t)$ is the first term in the (4.4) expression and $P_{NL}(\boldsymbol{r}, t)$ includes all remaining terms.

Let us assume that electromagnetic wave is quasi-monochromatic, so its spectral width $\Delta\omega$ is much smaller than frequency of the centre of wave packet ω_0 ($\Delta\omega / \omega_0 << 1$). This approximation is met for pulses of duration $\tau_0 > 0.1ps$, since the frequency of centre is of the order of $\omega_0 \approx 10^{-15}s$.

It is convenient to separate the fast varying part ω_0 and slowly varying with time the pulse envelope (slowly varying envelope approximation) and put down a wave as

$$E(\boldsymbol{r}, t) = \frac{1}{2}\hat{x}\left[E(\boldsymbol{r}, t)\exp(-i\omega_0 t) + c.c.\right] \tag{4.69}$$

and

$$\boldsymbol{P}_L(\boldsymbol{r}, t) = \frac{1}{2}\hat{x}\left[P_L(\boldsymbol{r}, t)\exp(-i\omega_0 t) + c.c.\right] \tag{4.70}$$

$$\boldsymbol{P}_{NL}(\boldsymbol{r}, t) = \frac{1}{2}\hat{x}\left[P_{NL}(\boldsymbol{r}, t)\exp(-i\omega_0 t) + c.c.\right] \tag{4.71}$$

where $\hat{x}$ is the unit polarization vector in x direction. Expressing polarization through the electric susceptibilities of the appropriate order in time domain $\chi_{xx}^{(1)}(t - t')$ and $\chi_{xxx}^{(3)}(t - t_1, t - t_2, t - t_3)$ we obtain

$$\boldsymbol{P}_L(\boldsymbol{r}, t) = \varepsilon_0 \int_{-\infty}^{\infty} \chi_{xx}^{(1)}(t - t')\boldsymbol{E}(\boldsymbol{r}, t')dt' \tag{4.72.a}$$

$$\boldsymbol{P}_{NL}(\boldsymbol{r}, t) = \varepsilon_0 \iint \int_{-\infty}^{\infty} \chi_{xxx}^{(3)}(t - t_1, t - t_2, t - t_3) \times \boldsymbol{E}(\boldsymbol{r}, t_1)\boldsymbol{E}(\boldsymbol{r}, t_2)\boldsymbol{E}(\boldsymbol{r}, t_3)dt_1 dt_2 dt_3 \tag{4.72.b}$$

and using (4.69) we get

$$P_L(\boldsymbol{r}, t) = \varepsilon_0 \int_{-\infty}^{\infty} \chi_{xx}^{(1)}(t - t')E(\boldsymbol{r}, t')\exp\left[i\omega_0(t - t')\right]dt'$$

$$= \frac{\varepsilon_0}{2\pi} \int_{-\infty}^{\infty} \tilde{\chi}_{xx}^{(1)}(\omega)\tilde{E}(\boldsymbol{r}, \omega - \omega_0)\exp\left[-i(\omega - \omega_0)t\right]d\omega \tag{4.73}$$

where $\tilde{\chi}_{xx}^{(1)}$ and $\tilde{E}(\boldsymbol{r}, \omega - \omega_0)$ denote the susceptibility and the electric field in the frequency domain after the Fourier transformation. We express $P_{NL}(\boldsymbol{r}, t)$ in the similar way. Generally, the response functions $\chi_{xxx}^{(3)}(t - t_1, t - t_2, t - t_3)$ are complex function of time. The nonlinear response of the system can be simplified significantly if we assume that the response is immediate. It is the drastic simplification because it is only electron polarization that is

immediate, vibrational degrees of freedom related to oscillations of molecule nuclei are much slower and the corresponding response of nuclei is not immediate after application of pulse of electric field. Obviously, this approximation can not be applied for description of the stimulated Raman scattering, because these are vibrations which decide about the Raman phenomenon. However, in first approximation, when we discuss the influence of pulses of time duration $\tau_0 > 0.1ps$ and we are not concerned of Raman effects, we can use that approximation. Then, the response function can be written

$$\chi^{(3)}_{xxx}(t-t_1, t-t_2, t-t_3) = \chi^{(3)}_{xxx}\delta(t-t_1)\delta(t-t_2)\delta(t-t_3) \tag{4.74}$$

where $\delta(t-t_1)$ function is the Dirac delta function (4.53)

The equation (4.72.b) takes the form of

$$\boldsymbol{P}_{NL}(\boldsymbol{r},t) = \varepsilon_0 \chi^{(3)} \times \boldsymbol{E}(\boldsymbol{r},t)\boldsymbol{E}(\boldsymbol{r},t)\boldsymbol{E}(\boldsymbol{r},t) \tag{4.75}$$

and if we use (4.71) we obtain

$$P_{NL}(\boldsymbol{r},t) \approx \varepsilon_0 \varepsilon_{NL} E(\boldsymbol{r},t) \tag{4.76}$$

where ε_{NL} denotes nonlinear contribution to dielectric constant

$$\varepsilon_{NL} = \frac{3}{4}\chi^{(3)}_{xxxx}\left|E(\boldsymbol{r},t)\right|^2 \tag{4.77}$$

After substitution (4.69) - (4.71) to (4.68) we obtain the Helmholz equation

$$\nabla^2 \tilde{E} + \varepsilon(\omega)k_0^2 \tilde{E} = 0 \tag{4.78}$$

where:

$$k_0 = \frac{\omega}{c};\ \varepsilon(\omega) = 1 + \tilde{\chi}^{(1)}_{xx}(\omega) + \varepsilon_{NL} \tag{4.79}$$

and

$$\tilde{E}(\boldsymbol{r}, \omega-\omega_0) = \int_{-\infty}^{\infty} E(\boldsymbol{r},t)\, exp\left[i(\omega-\omega_0)t\right]dt \tag{4.80}$$

To derive the Helmholtz equation for the nonlinear regime, additional assumption of ε_{NL} =const was needed, which is not generally valid due to the dependence on the field intensity. Let us assume that in the first approximation that due to slowly varying envelope approximation the approximation ε_{NL} =const employed in solving (4.68) is acceptable. Like in the linear approximation, the real and the imaginary part of dielectric constant depend on refraction coefficient $\tilde{n}$ and absorption coefficient $\tilde{\alpha}$

$$\varepsilon = (\tilde{n} + i\tilde{\alpha} / 2k_0)^2 \tag{4.81}$$

In the nonlinear regime the refraction coefficient $\tilde{n}$ and the absorption coefficient depend on field intensity and usually they take the form

$$\tilde{n} = n + n_2\left|E\right|^2 \quad , \quad \tilde{\alpha} = \alpha + \alpha_2\left|E\right|^2 \tag{4.82}$$

where

$$n_2 = \frac{3}{8n} Re\left(\chi^{(3)}_{xxxx}\right) \quad , \quad \alpha_2 = \frac{3\omega_0}{4nc} Im\left(\chi^{(3)}_{xxxx}\right) \tag{4.83}$$

Applying the method of variables separation, which we have already used in chapter 1 in order to solve the Helmholtz equation for the linear case, we can write the intensity of the field $\tilde{E}(r, \omega - \omega_0)$ as a product of the field component $F(x, y)$ in perpendicular plane to the propagation of wave, the component of slowly varying envelope in the z direction $\tilde{A}(z, \omega - \omega_0)$ and the fast varying component of $exp(i\beta_0 z)$

$$\tilde{E}(r, \omega - \omega_0) = F(x, y)\tilde{A}(z, \omega - \omega_0)\, exp(i\beta_0 z) \tag{4.84}$$

where β_0 is the wave vector (we called it the propagation constant in chapter 1) and is the first term in Taylor series expansion

$$\beta(\omega) = \beta_0 + (\omega - \omega_0)\beta_1 + \frac{1}{2}(\omega + \omega_0)^2 \beta_2 + \frac{1}{6}(\omega - \omega_0)^3 \beta_3 + ... \tag{4.85}$$

where

$$\beta_m = \left(\frac{d^m \beta}{d\omega^m} \right)_{\omega = \omega_0} \qquad (m = 1,2...) \tag{4.86}$$

Substituting (4.84) into Helmholtz equation (4.78) we obtain

$$\frac{\partial^2 F}{\partial x^2} + \frac{\partial^2 F}{\partial y^2} + \left[\varepsilon(\omega) k_0^2 - \tilde{\beta}^2 \right] F = 0 \tag{4.86 }$$

$$2i\beta_0 \frac{\partial \tilde{A}}{\partial z} + \left(\tilde{\beta}^2 - \beta_0^2 \right) \tilde{A} = 0 \tag{4.87}$$

We can determine the wave vector $\tilde{\beta}$ from the equation (4.86) analogously to the method shown in chapter 1, where we described the propagation of modes in optical waveguides.
Using (4.81), we can approximate the dielectric constant by

$$\varepsilon = (n + \Delta n)^2 \approx n^2 + 2n\Delta n \tag{4.88}$$

where Δn is a nonlinear term of the refraction index and it is expressed by the equation

$$\Delta n = n_2 \left| E^2 \right| + \frac{i\hat{\alpha}}{2k_0} \tag{4.89}$$

The equation (4.86) can be solved using the first-order perturbation theory. Namely, if $\varepsilon \approx n^2$, the equation (4.86) is a solution of F(*x*,*y*) for the mode distribution of HE_{11} in a single-mode optical waveguide that was described in chapter 1. Having solution of the zero-order, F(*x*,*y*), we insert the perturbation of $2n\Delta n$ to the equation (4.86) and solve it using the first-order perturbation method

$$\hat{\beta}(\omega) = \beta(\omega) + \Delta\beta \tag{4.90}$$

where

$$\Delta\beta = \frac{k_0 \int_{-\infty}^{\infty} \int \Delta n \left| F(x, y) \right|^2 dxdy}{\int_{-\infty}^{\infty} \int \left| F(x, y) \right|^2 dxdy} \tag{4.91}$$

One can calculate **E**(**r**,t) from the equation (4.69) and polarizations of $P_L(\boldsymbol{r}, t)$ and $P_{NL}(\boldsymbol{r}, t)$ from (4.72a) via substitution

$$\boldsymbol{E}(\boldsymbol{r}, t) = \frac{1}{2}\hat{x}\{F(x, y)A(z, t)\,exp[i(\beta_0 z - \omega_0 t)] + c.c\} \tag{4.92}$$

where A(*z*,*t*) is the inverse Fourier transform of $\tilde{A}(z, \omega - \omega_0)$

$$A(z,t) = \frac{1}{2\pi}\int_{-\infty}^{\infty}\tilde{A}(z,\omega-\omega_0)\exp[-i(\omega-\omega_0)t]d\omega. \tag{4.93}$$

$\tilde{A}(z, \omega - \omega_0)$ can be derived from the equation (4.87) that can be written as

$$\frac{\partial\tilde{A}}{\partial z} = i[\beta(\omega) + \Delta\beta - \beta_0]\tilde{A} \tag{4.94}$$

where $(\tilde{\beta}^2 - \beta_0^2)$ is substituted by $2\beta_0(\tilde{\beta} - \beta_0)$.

In order to transform $A(z, t)$ to the time domain, the inverse Fourier transform should be applied, (4.93), for both sides of (4.94) that leads to

$$\frac{\partial A}{\partial z} = -\beta_1\frac{\partial A}{\partial t} - \frac{i\beta_2}{2}\frac{\partial^2 A}{\partial t^2} + i\Delta\beta A \tag{4.95}$$

Using (4.89) in (4.91) we can calculate $\Delta\beta$ and insert it to (4.95). Finally, we get time-domain wave equation

$$\frac{\partial A}{\partial z} + \beta_1\frac{\partial A}{\partial t} + \frac{i\beta_2}{2}\frac{\partial^2 A}{\partial t^2} + \frac{\alpha}{2}A = i\gamma|A|^2 A \tag{4.96}$$

This equation is known as the nonlinear Schrödinger equation (NLS) and plays a significant role in description of GVD effects and nonlinearity of optical waveguides.

that includes the following effects:

- losses in optical waveguide – term $\frac{\alpha}{2}A$,
- group velocity of the centre of pulse - $\beta_1\frac{\partial A}{\partial t}$,
- dispersion of the group velocity GVD - $\frac{i\beta_2}{2}\frac{\partial^2 A}{\partial t^2}$,
- nonlinearity of optical waveguide $i\gamma|A|^2 A$

where

$$\gamma = \frac{n_2\omega_0}{cA_{eff}} \tag{4.97}$$

and

$$A_{eff} = \frac{\left(\int_{-\infty}^{\infty}\int|F(x, y)|^2 dxdy\right)^2}{\int\int|F(x, y)|^4 dxdy} \tag{4.98}$$

Typical values of the parameters in equation (4.96) in standard glass single-mode optical waveguides for 1.5 μm:

$n_2 \approx 2.6 \times 10^{-20} m^2 / W$; $A_{eff} \approx 20 - 100 \mu m^2$;
$\gamma \approx 1 - 10 W^{-1} / km$; $\beta_2 = -20 ps^2 / km$

4.8.2. Inclusion of the higher order nonlinear effects in the nonlinear Schrödinger equation

Despite its usefulness for description of light propagation in optical waveguides for pulses longer than 1ps, the Schrödinger equation (4.96) is insufficient for characterisation of nonlinear phenomena such as the stimulated Raman scattering (SRS), the stimulated Brillouin scattering (SBS), the self-phase modulation (SPM), the four-wave mixing. Furthermore, the inclusion of the third term, β_3, in Taylor expansion (4.85) is occasionally necessary.

Now, we will show the methods that include these effects. Generally, the response functions $\chi^{(3)}_{xxx}(t - t_1, t - t_2, t - t_3)$ are complex function of time. As we have shown in the previous chapter, the nonlinear response of a system can significantly be simplified if the immediate response is assumed

$$\chi^{(3)}_{xxx}(t - t_1, t - t_2, t - t_3) = \chi^{(3)}_{xxx}\delta(t - t_1)\delta(t - t_2)\delta(t - t_3) \qquad (4.99)$$

This is the drastic simplification since only electron polarisation is immediate, vibrations of molecule nuclei are much slower and the corresponding response to the applied electric field is not immediate This approximation definitely cannot be used for description of the stimulated Raman scattering, since these are vibrations that decide on the Raman scattering. The phenomenon can be included by the response function *R* [16]

$$\chi^{(3)}(t - t_1, t - t_2, t - t_3) = \chi^{(3)} R(t - t_1)\delta(t - t_2)\delta(t - t_3) \qquad (4.100)$$

where $R(t - t_1)$ is a nonlinear response function, normalized so that $\int_{-\infty}^{+\infty} R(t)dt = 1$. The expression (4.100) is only correct for non-resonance conditions.
Substituting (4.100) to (4.72b) we get

$$P_{NL}(r, t) = \varepsilon_0 \chi^{(3)} E(r, t) \int_{-\infty}^{t} R(t - t_1)|E(r, t_1)|^2 dt_1 \qquad (4.101)$$

Applying analogous procedure as we employed in chapter 3, one can show [17] that in the frequency domain the equation similar to the Helmholtz one can be derived

$$\nabla^2 \tilde{E} + n^2(\omega)k_0^2 \tilde{E} = -ik_0\alpha + \chi^{(3)} \frac{\omega^2}{c^2} \int \int_{-\infty}^{\infty} \tilde{R}(\omega - \omega_1) \times \tilde{E}(\omega_1, z)\tilde{E}(\omega_2, z)\tilde{E}^*(\omega_1 + \omega_2 - \omega, z)d\omega_1 d\omega \qquad (4.102)$$

where $\tilde{R}(\omega - \omega_1)$ is the Fourier transform of the response function of $R(t - t_1)$. Treating the right-hand expression as a perturbation, we can derive the expression for the mode distribution, F(*x*,*y*), and for the wave vector

$$\tilde{\beta}(\omega) = \beta(\omega) + \Delta\beta \qquad (4.103)$$

where $\Delta\beta$ is a perturbation, but it is not expressed by formula (4.91). Defining slowly varying function A(*z*,*t*) in the same way as in the equation (4.92) we get [17]

$$\frac{\partial A}{\partial z} + \frac{\alpha}{2} A + \beta_1 \frac{\partial A}{\partial t} + \frac{i\beta_2}{2} \frac{\partial^2 A}{\partial t^2} - \frac{\beta_3}{6} \frac{\partial^3 A}{\partial t^3} = i\gamma\left(1 + \frac{i}{\omega_0} \frac{\partial}{\partial t}\right)\left(A(z,t) \int_{-\infty}^{\infty} R(t') \left|A\left(z, t - t'\right)\right|^2 dt'\right)$$

(4.104)

The equation (4.104) is valid not only for the slowly varying envelope approximation used before, but also for the pulses as short as several optical cycles.

The response function, $R(t)$, can be written as follows

$$R(t) = (1 - f_R)\delta(t) + f_R h_R(t) \tag{4.105}$$

where the first term describes immediate polarisation from electronic contribution, and the second term, f_R , depicts contribution of polarisation coming from vibrations. The function of $h_R(t)$ is connected with the Raman amplification described in chapter 4.3.

$$g_R(\Delta\omega) = \frac{\omega_0}{cn_0} f_R \chi^{(3)} Im\left[\tilde{h}_R(\Delta\omega)\right] \tag{4.106}$$

where Im corresponds to the imaginary part of the Fourier transform $\tilde{h}_R$ of the response function of $h_R(t)$. The real term can be derived from the imaginary one using Kramers-Kronig relation [18]. Applying various models for vibrations one can derive the analytical form of the $h_R(t)$. Below, the form of $h_R(t)$ for dumped oscillations is presented [19]

$$h_R(t) = \frac{\tau_1^2 + \tau_2^2}{\tau_1 \tau_2^2} exp\left(\frac{-t}{\tau_2}\right) sin\left(\frac{t}{\tau_1}\right) \tag{4.107}$$

The equation 4.104 can be simplified if we assume that pulses are short ($\tau_0 < 5ps$), however noticeably longer than the time interval of just few optical cycles ($\tau_0 >> 10fs$). Then expansion into Taylor series can be applied

$$\left|A\left(z, t - t'\right)\right|^2 \approx \left|A(z,t)\right|^2 - t' \frac{\partial}{\partial t} \left|A(z,t)\right|^2 \tag{4.108}$$

Defining the first moment of the response function as

$$T_R \equiv \int_{-\infty}^{\infty} tR(t)dt = f_R \int_{-\infty}^{\infty} th_R(t)dt = f_R \frac{d\left(Im\ \tilde{h}_R\right)}{d(\Delta\omega)}\Big|_{\Delta\omega=0} \tag{4.109}$$

and taking into account the fact that $\int_{-\infty}^{+\infty} R(t)dt = 1$ we get the equation after inserting (4.108) into (4.109)

$$\frac{\partial A}{\partial z} + \frac{\alpha}{2} A + \frac{i\beta_2}{2} \frac{\partial^2 A}{\partial T^2} - \frac{\beta_3}{6} \frac{\partial^3 A}{\partial T^3} = i\gamma\left(|A|^2 A + \frac{i}{\omega_0} \frac{\partial}{\partial T}\left(|A|^2 A\right) - T_R A \frac{\partial |A|^2}{\partial T}\right) \tag{4.110}$$

This equation is expressed in the reference system that moves with the group velocity, υ_g, of the centre of the wave packet where

$$T = t - \frac{z}{\upsilon_g} \equiv t - \beta_1 z \tag{4.111}$$

When comparing the equation 4.110 with the nonlinear Schrödinger equation (NLS) (4.96), we can notice three new terms, which are responsible for

- $\frac{\beta_3}{6}\frac{\partial^3 A}{\partial T^3}$ - introduces the third order dispersion. The inclusion of this dispersion turned out to be necessary for short pulses since they represent a very broad spectrum,
- $\frac{i}{\omega_0}\frac{\partial}{\partial T}\left(|A|^2 A\right)$ - introduces the first derivative of nonlinear polarization and it is responsible for self-steeping and shock formation [20]
- $T_R A \frac{\partial |A|^2}{\partial T}$ is connected with Raman effect. It is responsible for the self-frequency shift [21] and it is induced by intrapulse scattering.

In practice, when a pulse duration $\tau_0 > 5ps$, the last two terms are negligible. Moreover, the first term is also insignificant if the wavelength of the pulse centre is not close to the wavelength, where the dispersion coefficient D=0. Therefore, we can write

$$i\frac{\partial A}{\partial z} + \frac{i\alpha}{2}A - \frac{\beta_2}{2}\frac{\partial^2 A}{\partial T^2} + \gamma|A|^2 A = 0 \tag{4.112}$$

This equation is similar to the nonlinear Schrödinger equation (4.96), if the moving reference system is applied, (4.111).

When the peak-power of pulses reaches the order of 1GW/cm^2, fifth-order nonlinear terms should be included in (4.4). This effect can be included through replacement of γ parameter in (4.112) by the modified parameter

$$\gamma = \frac{\gamma_0 A}{1 + b_s|A|^2} \approx \gamma_0\left(1 - b_s|A^2|\right) \tag{4.113}$$

where b_s denotes the saturation parameter. In practice, for glass optical waveguides $b_s|A|^2 << 1$ and equation 4.112 can successfully be used even in case of relatively high peak-powers. However if saturation effect exists, we take it into account through inclusion (4.113) into the equation (4.112). Such equation is named the cubic-quintic NLS equation.

4.8.3. The derivation of formula for pulse broadening due to the GVD effect [15]

In chapter 3 we showed that the group velocity dispersion, GVD, causes pulse broadening. In that chapter, we will derive the formulas that were used in chapter 3.

The analysis will be confined to pulses longer than $\tau_0 > 5ps$, so the nonlinear Schrödinger equation (4.112) can be applied

$$i\,\frac{\partial A}{\partial z} = -\frac{i\alpha}{2}\,A + \frac{\beta_2}{2}\,\frac{\partial^2 A}{\partial T^2} - \gamma|A|^2 A \qquad (4.114)$$

As we said in chapter 4.8.2, this equation includes

- loses in an optical waveguide – term $\frac{\alpha}{2}\,A$,
- group velocity – it was the term $\beta_1\,\frac{\partial A}{\partial t}$ in eq. (4.96) that was taken into account in (4.114) via introduction the moving reference system

  $T = t - \frac{z}{\upsilon_g} \equiv t - \beta_1 z$
- group velocity dispersion, GVD, $\frac{\beta_2}{2}\,\frac{\partial^2 A}{\partial T^2}$,
- nonlinearity of optical waveguide, $\gamma|A|^2 A$

Let us introduce normalized the time scale with respect to the input pulse duration τ_0

$$\tau = \frac{T}{\tau_0} = \frac{t - \frac{z}{\upsilon_g}}{\tau_0} \qquad (4.115)$$

and the normalized pulse amplitude, $U(z,\tau)$, that is independent of loses in an optical waveguide

$$A(z,\tau) = \sqrt{P_0}\ exp(-\alpha z/2)U(z,\tau) \qquad (4.116)$$

where P_0 denotes power of the input pulse.
Using relations of (4.115-4.116) in 4.114 we get

$$i\,\frac{\partial U}{\partial z} = \frac{sgn(\beta_2)}{2L_D}\,\frac{\partial^2 U}{\partial \tau^2} - \frac{exp(-\alpha z)}{L_{NL}}\,|U|^2 U \qquad (4.117)$$

where $sgn(\beta_2) = \pm 1$ represemts the sign of (β_2) parameter that characterises GVD, and

$$L_D = \frac{\tau_0^2}{|\beta_2|},\ L_{NL} = \frac{1}{\gamma P_0}. \qquad (4.118)$$

L_D and L_{NL} is known in literature as the dispersion length and the nonlinear length, respectively and characterize the optical length L of a fiber, for which dispersion effects and nonlinear effects are negligible (4.117)

- if the length of optical waveguide fulfils the condition of $L << L_D$ and $L << L_{NL}$, both the group velocity dispersion effects, GVD, and the nonlinear effects can be neglected,
- if $L << L_{NL}$ but $L \approx L_D$, the nonlinear effects are negligible, but GVD is important resulting in temporal pulse broadening,
- if $L << L_D$ but $L \approx L_{NL}$, the dispersion effects are negligible in comparison to the nonlinear effects, time pulse distortion is caused by the self-phase modulation, SPM.

Of course the first case, when both GVD and SMP effects are negligible, is the most desirable case for optical transmission. We can estimate L_D and L_{NL} from eq. (4.118) for certain input powers P_0 and duration of pulses τ_0, assuming typical values of $|\beta_2| \approx 20 ps^2 / km$ and $\gamma \approx 3 W^{-1} km^{-1}$ in the window of 1550nm. For short pulses and low input powers P_0, i.e. $P_0 << 1W$, $\tau_0 \approx 1ps$, the second case with GVD dominates with

$$\frac{L_D}{L_{NL}} = \frac{\gamma P_0 \tau_0^2}{|\beta_2|} << 1 \tag{4.119}$$

For longer pulses and high input powers P_0, e.g. $P_0 \approx 1W$, the self-phase modulation SMP dominates

$$\frac{L_D}{L_{NL}} = \frac{\gamma P_0 \tau_0^2}{|\beta_2|} >> 1. \tag{4.120}$$

Summarizing this part of discussion we can say that

for standard telecommunications optical waveguides of the length of 50-80km in the window of 1550nm $|\beta_2| \approx 20 ps^2 / km$ and pulses of τ_0 >100ps, $L_D \approx 500 km$, the dispersion effects, GVD, are negligible ($L << L_D$). However for shorter pulses of τ_0 of the order of 1 ps, $L_D \approx 50 m$, the dispersion effect is not negligible since $L >> L_D$.

Let us consider now the influence of GVD dispersion on the pulse broadening. In chapter 3 we showed that the group velocity dispersion, GVD, causes pulse broadening (3.27a). Now we will derive that expression and other formulas, which are useful in analysis of pulse distortion caused by GVD dispersion. Let us neglect the influence of nonlinearity, SPM, inserting γ=0 into (4.114) and (4.117) we obtain

$$i \frac{\partial U}{\partial z} = \frac{\beta_2}{2} \frac{\partial^2 U}{\partial T^2} \tag{4.121}$$

The equation can simply be solved in the frequency domain, if we use the inverse Fourier transform

$$U(z,T) = \frac{1}{2\pi} \int_{-\infty}^{\infty} \tilde{U}(z,\omega) \exp(-i\omega T) d\omega \tag{4.122}$$

Using (4.122) in (4.121) we get the equation

$$i \frac{\partial \tilde{U}}{\partial z} = -\frac{1}{2} \beta_2 \omega^2 \tilde{U} \tag{4.123}$$

with the solution

$$\tilde{U}(z,\omega) = \tilde{U}(0,\omega) \exp\left(\frac{i}{2} \beta_2 \omega^2 z\right) \tag{4.124}$$

The expression (4.124) illustrates that the dispersion effect, GVD, causes phase shift of each frequency separately. The magnitude of that shift depends on the optical path z of a pulse propagating in an optical fiber. Coming back to the time domain (4.122) and substituting (4.124) we obtain

$$U(z,T) = \frac{1}{2\pi} \int_{-\infty}^{\infty} \tilde{U}(0,\omega)\, exp\left(\frac{i}{2}\, \beta_2 \omega^2 z - i\omega T \right) d\omega \tag{4.125}$$

where $\tilde{U}(0,\omega)$ is the normalized amplitude of the input pulse for *z=0* in the frequency domain and is expressed via the Fourier transform

$$\tilde{U}(0,\omega) = \int_{-\infty}^{\infty} U(0,T)\, exp(i\omega T) dT \tag{4.126}$$

Let us assume the incident pulse has the Gaussian shape

$$U(0,T) = exp\left(- \frac{T^2}{2\tau_0^2} \right) \tag{4.127}$$

where τ_0 the is pulse duration defined as the half-width for the intensity corresponding to 1/e of its maximal value and is related to the full width at half maximum through the relation of

$$T_{FWHM} = 2(ln\ 2)^{\frac{1}{2}} \tau_0 \approx 1.665\tau_0 \tag{4.128}$$

Using (4.127) in (4.126) and (4.125) we get

$$U(z,T) = \frac{\tau_0}{\left(\tau_0^2 - i\beta_2 z\right)^{\frac{1}{2}}}\, exp\left(- \frac{T^2}{2\left(\tau_0^2 - i\beta_2 z\right)} \right) \tag{4.129}$$

Comparing (4.127) with (4.129) we can state that the pulse keeps the Gaussian shape but it exhibits broadening

$$\tau(z) = \tau_0 \left[1 + \left(\frac{z}{L_D} \right)^2 \right]^{\frac{1}{2}} \tag{4.130}$$

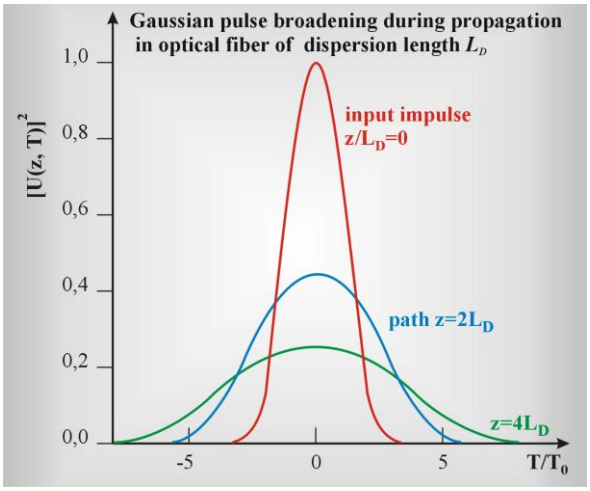

Fig. 4.28. Illustration of a Gaussian pulse broadening during propagation in an optical fiber ---- incident pulse at $z=0$, 2 – pulse after the length of $z=2L_D$, 4 – pulse after the length of $z=4L_D$ [21], where L_D denotes dispersion length of fiber defined by the expression of (4.118).

The incident unchirped pulse does not show the phase modulation, however the pulse propagating through an optical fiber begins to exhibit the phase modulation. Indeed, comparing (4.127) with (4.129) we get

$$U(z,T) = |U(z,T)|\, exp[i\phi(z,T)] \tag{4.131}$$

where the phase of $\phi(z,T)$ depends on time and is expressed by the formula

$$\phi(z,T) = -\frac{sgn(\beta_2)\left(\frac{z}{L_D}\right)}{1+\left(\frac{z}{L_D}\right)^2}\frac{T^2}{\tau_0^2} + \frac{1}{2}\,tan^{-1}\left(\frac{z}{L_D}\right), \tag{4.132}$$

and

$$\delta\omega(T) = -\frac{\partial\Phi}{\partial T} = \frac{sgn(\beta_2)\left(\frac{2z}{L_D}\right)}{1+\left(\frac{z}{L_D}\right)^2}\frac{T}{\tau_0^2} \tag{4.133}$$

The expression (4.133) denotes that the frequency changes linearly on T. If $\beta_2>0$ (positive GVD effect) $\delta\omega(T)<0$ for T<0 for the leading edge of the time pulse, and positive for T>0 for the trailing edge. It means that the longer spectral components of the pulse travel faster than the shorter components and are in front of the temporal pulse. When an optical fiber shows negative GVD effect, blue components are in front of pulse and red ones at its end. Independently on the sign of GVD, the effect GVD causes pulse broadening (4.130) (Fig. 4.27).

The situation is a bit different when the incident pulse has already got an initial chirp [21]. The initial chirp can be included through C parameter

$$U(0,T) = exp\left(-\frac{(1+iC)}{2}\frac{T^2}{\tau_0^2}\right) \tag{4.134}$$

When calculating $\delta\omega(T) = -\frac{\partial\Phi}{\partial T}$ one can state that for C>0 the change of frequency $\delta\omega(T)$ rises linearly till the trailing edge (up-chirp), and it is opposite for C<0 (down-chirp). It indicates that C>0 denotes the positive chirp and C<0 – the negative chirp. Inserting (4.134) into (4.126) we get

$$\tilde{U}(0,\omega) = \left(\frac{2\pi\tau_0^2}{1+iC}\right)^{\frac{1}{2}} exp\left(-\frac{\omega^2\tau_0^2}{2(1+iC)}\right) \tag{4.135}$$

with the spectral width (1/e) equal to

$$\Delta\omega = (1+C^2)^{\frac{1}{2}} / \tau_0. \tag{4.136}$$

For C=0 the condition of $\Delta\omega\tau_0$=1 is met, the Fourier transform-limited case occurs and the pulse exhibits no chirp. Inserting (4.135) into (4.125) we obtain the pulse that remains Gaussian

$$U(z,T) = \frac{\tau_0}{\left[\tau_0^2 - i\beta_2 z(1+iC)\right]^{\frac{1}{2}}} exp\left(-\frac{(1+iC)T^2}{2\left[\tau_0^2 - i\beta_2 z(1+iC)\right]}\right), \tag{4.137}$$

and the pulse duration changes according to the relation

$$\frac{\tau}{\tau_0} = \left[\left(1+\frac{C\beta_2 z}{\tau_0^2}\right)^2 + \left(\frac{\beta_2 z}{\tau_0^2}\right)^2\right]^{\frac{1}{2}} \tag{4.138}$$

The time duration of the pulse depends on the sign of the initial chirp, C, and the sign of GVD dispersion in the optical fiber. If $C\beta_2$>0, the time pulse undergoes monotonic broadening with the increase in optical distance, z. If $C\beta_2$<0, the duration of the pulse decreases first and then monotonically increases with the increase in optical distance, z.

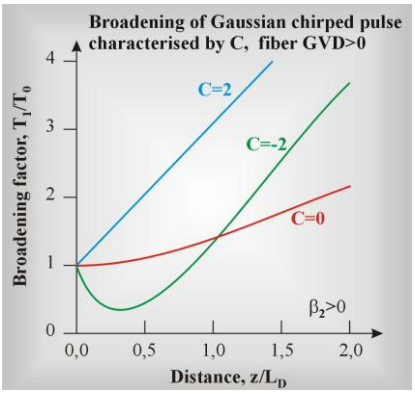

Fig. 4.29. Broadening of Gaussian chirped pulse characterised by C parameter during propagation in optical waveguide of positive dispersion, GVD>0, ----- pulse for C=0, C=2 – pulse with input positive GVD dispersion, C=-2 pulse with input negative GVD dispersion [21]. When a fibre shows GVD<0 the same curves characterize bandwidth broadening when we change signs of C.

It is easy to understand the initial effect of pulse shortening looking at (4.138) equation. If $C\beta_2$ <0 at the input, a pulse shows its own negative GVD (characterized by C parameter) opposite to GVD of the fiber in which it starts to propagate. It means that shorter wavelengths, which travelled faster at the input, start to demonstrate a delay effect and longer wavelengths starts to travel faster down the fiber. It leads to compensation of the GVD dispersion effect. The pulse reaches minimum for such the distance of z_{min} in optical waveguide when both effects are compensated (GVD = 0). The distance can be derived form the (4.138) expression

$$z_{\min} = \frac{|C|}{1+C^2} L_D \tag{4.139}$$

For $z_{\min}$ the pulse is the shortest $\tau_{\min}$ and it shows transform-limited spectral band width, $\Delta\omega$,

$$\tau_{min} = \frac{\tau_0}{(1 + C^2)^{1/2}} \tag{4.140}$$

where $\Delta\omega \cdot \tau_{\min} = 1.$

When the pulse propagates further, for distances longer than z_{min} GVD effect of the optical waveguide starts to dominate and the pulse becomes exhibit broadening again.

Now, we will return to the analysis of the self-phase modulation (SPM). As we said in chapter 3 this effect comes from the fact that the nonlinear refraction coefficient $n_2(\omega)$ depends on pulse intensity $I(t)$

$$n(\omega) = n_0(\omega) + n_2(\omega)I(t). \tag{4.141}$$

Let us assume that GVD is negligible. In eq. (4.117) we can put $\beta_2 = 0$ to obtain

$$\frac{\partial U}{\partial z} = \frac{ie^{-\alpha z}}{L_{NL}} |U^2| U \tag{4.142}$$

where U is the normalized amplitud defined by (4.116), L_{NL} is the nonlinear length

$$L_{NL} = (\gamma P_0)^{-1} \tag{4.143}$$

where γ depends on the nonlinear refraction index n_2 (4.141), P_o is the peak power of the puls. Equation (4.142) can be easily solved substituting $U = V\, exp(i\phi_{NL})$ where ϕ_{NL} is nonlinear phase (4.47b). We get

$$\frac{\partial V}{\partial z} = 0 \quad , \quad \frac{\partial \phi_{NL}}{\partial z} = \frac{e^{-\alpha z}}{L_{NL}} V^2 \tag{4.150}$$

The solution of eq.(4.142) is constant, the integral over the length *L* is

$$U(L,T) = U(0,T)\,exp[i\phi_{NL}(L,T)] \tag{4.151}$$

where U(*0,T*) is the normalized amplitude for *z=0,* the nonlinear phase ϕ_{NL} for *z=L* is obtained as

$$\phi_{NL}(L,T) = |U(0,T)|^2 (L_{eff} \;/\; L_{NL}) \tag{4.152}$$

where the effective length L_{eff} is defined as

$$L_{eff} = [1 - exp(-\alpha L)] \;/\; \alpha \tag{4.153}$$

Maximum of nonlinear phase is in the center of the temporal pulse (*T=0*), because we showed that ϕ_{NL} depends on the intensity. Thus, for the amplitude normalized as U(*0,0*)=1, we get

$$\Phi_{max} = \frac{L_{eff}}{L_{NL}} = \gamma P_0 L_{eff} \tag{4.154}$$

As we showed in chapter 4.6 the spectral broadening of the pulse δ_ω due to SMP comes from the time dependence of nonlinear phase ϕ_{NL}. The transient frequency $\delta\omega(T) = \omega - \omega_0$ along the pulse can be calculated from

$$\delta\omega(T) = -\frac{\partial\phi_{NL}}{\partial T} = -\left(\frac{L_{eff}}{L_{NL}}\right)\frac{\partial}{\partial T}|U(0,T)|^2 \tag{4.155}$$

The temporal broadening depends on the shape of U(*0.T*). Let us assume that the shape is given by

$$U(0,T) = exp\left[-\frac{1+iC}{2}\left(\frac{T}{z_0}\right)^{2m}\right] \tag{4.156}$$

Substituting (4.156) into (4.155) we get

$$\delta\omega(T) = \frac{2m}{T_0}\,\frac{L_{eff}}{L_{NL}}\left(\frac{T}{T_0}\right)^{2m-1} exp\left[-\left(\frac{T}{T_0}\right)2m\right] \tag{4.157}$$

From (4.157) one can see that for T<0 (leading edge of the pulse), $\delta_\omega < 0$ (red shift), for T=0 (puls center), $\delta_\omega = 0$, for T>0 (trailing edge), $\delta\omega > 0$ (blue shift).

Derived here formulas help to understand the phase modulation (frequency chirp) shown in Fig. 4.21 which illustrates the principle of automodulation SPM.

1. R.H. Stolen, E.P. Ippen, Raman gain in glass optical waveguides, Appl. Phys. Lett. Vol.22, no.6, 1973
2. 3.V. V. Raman and K. S. Krishnan, "A new type of secondary radiation", Nature 121, 501-2 (1928)
3. J. Hecht, Raman amplifiers boost system margins at high speed, Laser Focus World 37(6) (June, 2001) 135-140
4. J. Hecht, Mitigating nonlinear effects is essential to long-haul transmission systems, Laser Focus World 38(5) (May, 2002) 155-162
5. M. Islam, M. Nietubyc, Not a pretty picture, WDM solutions 3(3) (March 2001)
6. Halina Abramczyk, Introduction to Laser Spectroscopy, Elsevier, New York, 2005
7. M. N. Islam, IEEE Journal of selected Topics in Quantum Electronics, vol.8, no. 3, 2002
8. Y. R. Shen, The principles of Nonlinear Optics, Wiley, New York, 1984, chap. 10
9. R. G. Smith, Appl. Opt. 11, 2489 (1972)]
10. G. P. Agrawal, Nonlinear fiber optics, 3rd edition, Academic Press, 2001, p. 361
11. R. H. Stolen, C. Lin, Phys. Rev. A 17, 1448 (1978)]
12. G. P. Agrawal, Nonlinear fiber optics, 3rd edition, Academic Press, 2001, p. 104
13. G. P. Agrawal, Nonlinear fiber optics, 3rd edition, Academic Press, 2001, p.105
14. S. Mukamel, Principles of Nonlinear Spectroscopy, Oxford, 1995
15. G. P. Agrawal, Nonlinear fiber optics, 3rd edition, Academic Press, 2001
16. K.J. Blow, D. Wood, IEEE J. Quantum Electron. 25, 2665 (1989)]
17. P.M. Mamyshev, S. V. Chernikov, Opt. Lett. 15, 1076 (1990)]
18. M.Schubert, B. Wilhelmi, Nonlinear Optics and Quantum Electronics, Wiley, New York, 1986
19. K.J. Blow, D. Wood, IEEE J. Quantum Electron. 25, 2665 (1989)]
20. S. Blair, K. Wagner, Opt. Quantum Electron. 30, 697 (1998)
21. G. P. Agrawal, "Nonlinear fiber optics", 3rd edition, Academic Press, 2001